Eur. Phys. J. C (2024) 84:742
https://doi.org/10.1140/epjc/s10052-024-12979-0

THE EUROPEAN PHYSICAL JOURNAL C

Regular Article - Experimental Physics

Search for short- and long-lived axion-like particles in $H \to aa \to 4\gamma$ decays with the ATLAS experiment at the LHC

ATLAS Collaboration[*]

CERN, 1211 Geneva 23, Switzerland

Received: 7 December 2023 / Accepted: 2 June 2024
© CERN for the benefit of the ATLAS Collaboration 2024

Abstract Presented is the search for anomalous Higgs boson decays into two axion-like particles (ALPs) using the full Run 2 data set of 140 fb^{-1} of proton-proton collisions at a centre-of-mass energy of 13 TeV recorded by the ATLAS experiment. The ALPs are assumed to decay into two photons, providing sensitivity to recently proposed models that could explain the $(g-2)_\mu$ discrepancy. This analysis covers an ALP mass range from 100 to 62 GeV and ALP-photon couplings in the range $10^{-7}\,\text{TeV}^{-1} < C_{a\gamma\gamma}/\Lambda < 1\,\text{TeV}^{-1}$, and therefore includes signatures with significantly displaced vertices and highly collinear photons. No significant excess of events above the Standard Model background is observed. Upper limits at 95% confidence level are placed on the branching ratio of the Higgs boson to two ALPs in the four-photon final state, and are in the range of 10^{-5} to 3×10^{-2}, depending on the hypothesized ALP mass and ALP-photon coupling strength.

Contents

1 Introduction . . . .
2 The ATLAS detector . . . .
3 Data set and simulated events . . . .
4 Object reconstruction and event selection . . . .
4.1 Object reconstruction . . . .
4.2 Event selection and categorization . . . .
5 Background estimation . . . .
5.1 Two-photon final states in the search for long-lived axion-like particles . . . .
5.2 Three- and four-photon final states in the search for long-lived axion-like particles . . . .
5.3 Four-photon final states in the search for promptly decaying axion-like particles . . . .
5.4 Background estimate summary . . . .
6 Systematic uncertainties . . . .
6.1 General experimental uncertainties . . . .
6.1.1 Uncertainties due to displaced ALP decays
6.2 Uncertainties on the background estimation . . .
6.3 Impact of theory uncertainties . . . .
7 Results . . . .
8 Conclusion . . . .
References . . . .

1 Introduction

Axion-like particles (ALPs), or more generally light (pseudo) scalars, are represented as gauge-singlets beyond the Standard Model (SM) that can couple to the 125 GeV Higgs boson [1,2], and appear in many well-motivated extensions of the SM, e.g., the next-to-minimal supersymmetric standard model [3,4]. These include models that address the baryon asymmetry of the universe [5,6], offer a solution to the naturalness problem [7,8], or provide insights into the nature of dark matter [9–14]. ALPs and light bosons produced in Higgs boson decays could also be mediators to dark sectors that do not otherwise couple to the SM [15].

A combination of ATLAS measurements of Higgs boson properties using 139 fb^{-1} of data constrains the branching ratios into invisible and undetected states to be $\mathcal{B}(H \to \text{invisible}) < 10.7\%$ and $\mathcal{B}(H \to \text{undetected}) < 12\%$ at 95% confidence level (CL) [16,17]. Combined measurements of Higgs boson couplings performed by the CMS Collaboration using 138 fb^{-1} of data set upper limits of $\mathcal{B}(H \to \text{invisible}) < 16\%$ and $\mathcal{B}(H \to \text{undetected}) < 16\%$ at 95% CL [18]. These results allow potentially large branching fractions into beyond-the-standard-model (BSM) particles, $\mathcal{B}(H \to \text{BSM})$, such as ALPs.

In Ref. [19] it has been argued that if the ALP, denoted as a in the following, couples to at least some SM particles with couplings of order (0.01–1)TeV^{-1}, its mass must be above 1 MeV. Taking into account the possibility of a long-lived ALP, large regions of so far unconstrained parameter space can be explored by searches for exotic, on-shell Higgs boson decays into two ALPs. In particular, this includes the parameter space in which ALPs can explain the observed discrep-

[*] e-mail: atlas.publications@cern.ch

Published online: 26 July 2024

ancy between the measurement [20–22] and the theoretical prediction [23,24] of the anomalous magnetic moment of the muon [19]. It was suggested that subsequent ALP decays into photons provide unprecedented sensitivity to the ALP-photon couplings in the mass region above a few MeV, even if the relevant ALP-photon couplings are loop suppressed and the $a \to \gamma\gamma$ branching ratios are significantly less than 100% [19].

This paper presents a search for decays of the 125 GeV Higgs boson into two ALPs in proton–proton (pp) collisions at the LHC [25]. The search is sensitive to events where each a-boson decays into two photons. For the first time, a dedicated search for long-lived $a \to \gamma\gamma$ decays with a significantly displaced vertex within the tracking system of the ATLAS detector is performed, allowing a large region of the parameter space of the ALP-photon coupling $C_{a\gamma\gamma}$ to be probed. Previous searches for $H \to aa \to 4\gamma$ signatures were performed by the ATLAS [26] and CMS Collaborations [27,28], but assumed promptly decaying ALPs and hence were valid only up to decay lengths of a few centimeters. The decay length scales with $\tau_a \propto \Lambda^2/\left(m_a^3|C_{a\gamma\gamma}|^2\right)$, where m_a is the ALP mass and Λ, the new physics scale, is assumed to be in the TeV range [19]. The limits obtained here for ALP masses $m_a > 15$ GeV are about one order of magnitude more stringent than previous ATLAS analyses using 8 TeV data, and reach sensitivities similar to or slightly better than previous analyses from CMS using 132 fb^{-1} of $\sqrt{s} = 13$ TeV data.

The paper is structured as follows. A brief discussion of the ATLAS detector and an overview of the Monte Carlo (MC) samples and data sets used are given in Sects. 2 and 3. Object reconstruction and the event selection are described in Sect. 4, where special focus is given to the reconstruction of collimated photon signatures and to the categorization of the final state topologies that can be reconstructed in the detector. The background estimates are discussed in Sect. 5, followed by a description of the dominant systematic uncertainties in Sect. 6, in particular those that involve the reconstruction of photons with a displaced production vertex. The statistical interpretation and the final results are summarized in Sect. 7. The paper closes with a brief conclusion in Sect. 8.

2 The ATLAS detector

The ATLAS detector [29] at the LHC covers nearly the entire solid angle around the collision point.[1] It consists of an inner tracking detector surrounded by a thin superconducting solenoid, electromagnetic and hadron calorimeters, and a muon spectrometer incorporating three large superconducting air-core toroidal magnets.

The inner-detector system (ID) is immersed in a 2 T axial magnetic field and provides charged-particle tracking in the range of $|\eta| < 2.5$. The high-granularity silicon pixel detector covers the vertex region and typically provides four measurements (hits) per track, the first hit normally being in the insertable B-layer (IBL) installed before Run 2 [30,31]. It is followed by the silicon microstrip tracker (SCT), which usually provides eight measurements per track. These silicon detectors are complemented by the transition radiation tracker (TRT), which enables radially extended track reconstruction up to $|\eta| = 2.0$. The TRT also provides electron identification information based on the fraction of hits (typically 30 in total) above a higher energy-deposit threshold corresponding to transition radiation.

The calorimeter system covers the pseudorapidity range of $|\eta| < 4.9$. Within the region $|\eta| < 3.2$, electromagnetic calorimetry is provided by barrel and endcap high-granularity lead/liquid-argon (LAr) calorimeters, with an additional thin LAr presampler covering $|\eta| < 1.8$ to correct for energy loss in material upstream of the calorimeters. Hadron calorimetry is provided by the steel/scintillator-tile calorimeter, segmented into three barrel structures within $|\eta| < 1.7$, and two endcap copper/LAr hadron calorimeters up to $|\eta| < 3.2$. The solid angle coverage is completed with forward copper/LAr and tungsten/LAr calorimeter modules optimised for electromagnetic and hadronic energy measurements, respectively.

The muon spectrometer (MS) comprises separate trigger and high-precision tracking chambers that measure the deflection of muons in the magnetic field generated by the superconducting air-core toroidal magnets. The field integral of the toroids ranges between 2.0 and 6.0 Tm across most of the detector. Three layers of precision chambers, each consisting of layers of monitored drift tubes, cover the region $|\eta| < 2.7$, complemented by cathode-strip chambers in the forward region. The muon trigger system covers the range of $|\eta| < 2.4$ with resistive-plate chambers in the barrel, and thin-gap chambers in the endcap regions.

Events of interest for this analysis are selected using dedicated di-photon triggers. The first-level of the trigger system is implemented in custom hardware, followed by a high-level trigger [32] where further selections are made by algorithms implemented in software. The first-level trigger accepts events from the 40 MHz bunch crossings at a rate below 100 kHz, which the high-level trigger further reduces in order to record events to disk at about 1 kHz.

[1] ATLAS uses a right-handed coordinate system with its origin at the nominal interaction point (IP) in the centre of the detector and the z-axis along the beam pipe. The x-axis points from the IP to the centre of the LHC ring, and the y-axis points upwards. Cylindrical coordinates (r, ϕ) are used in the transverse plane, ϕ being the azimuthal angle around the z-axis. The pseudorapidity is defined in terms of the polar angle θ as $\eta = -\ln\tan(\theta/2)$. Angular distance is measured in units of $\Delta R \equiv \sqrt{(\Delta\eta)^2 + (\Delta\phi)^2}$.

An extensive software suite [33] is used in MC simulation, in the reconstruction and analysis of real and simulated data, in detector operations, and in the trigger and data acquisition systems of the experiment.

3 Data set and simulated events

This analysis uses pp collision data collected by the ATLAS experiment from 2015 to 2018 with a centre-of-mass energy of $\sqrt{s} = 13$ TeV. After data quality requirements [34] the full data set corresponds to an integrated luminosity of 140.1 ± 1.2 fb^{-1} [35]. The lowest-threshold unprescaled diphoton triggers are used to select events for further analysis, as discussed in Sect. 4.2.

The main background contributions stem from multijet processes, where jets might be misidentified as photons, as well as Standard Model multiphoton processes [36]. However, MC simulation does not capture the full background shape observed in data and therefore a fully data-driven background estimation has been employed. Simulated events are used to validate the data-driven background estimation techniques described in Sects. 5.1–5.2, and to model Higgs boson decays into photons for both signal and background processes. Background events from continuum 3γ, 4γ and $\gamma\gamma$ production, neglecting any interference effects with the $H \to \gamma\gamma$ decay, are generated using Sherpa 2.2.8 and Sherpa 2.2.4 [37–39], respectively, with the AZNLO set of tuned parameters [40] and the NNPDF30 [41] set of parton distribution functions (PDF). Production of the Higgs boson through gluon–gluon fusion (ggF) and vector-boson fusion (VBF) processes is modelled at next-to-leading order (NLO) using POWHEG- BOX v2 [42–44] interfaced with PYTHIA 8.186 [45] using the AZNLO tune and NNPDF30 PDF. The change in selection efficiency between ggF and VBF and other Higgs boson production mechanisms is at the percent level, so its impact is negligible. Thus, all signal ($H \to aa \to 4\gamma$) samples use the ggF Higgs boson production mechanism and have their cross-sections scaled to the total Higgs boson production cross-section predicted by a next-to-next-to-next-to-leading-order QCD calculation with NLO electroweak corrections applied [46–49].

Signal samples are produced for ALP masses in the range of 0.1 GeV–62 GeV, with a spacing of 0.1 GeV in the range of 0.1 GeV–0.5 GeV, a spacing of 0.5 GeV in the range of 0.5 GeV–5 GeV and a spacing of 1 GeV in the range of 5 GeV–62 GeV, assuming $\Lambda = 1$ TeV. The full set of mass points is simulated for four different values of the coupling $C_{a\gamma\gamma}$: $1, 0.01, 5 \times 10^{-4}$ and 10^{-5}. Samples of simulated signal events are generated using POWHEG- BOX v2 at NLO for the Higgs production and PYTHIA 8.212 to simulate the decay into ALPs and the subsequent decay into photons employing a generic 2HDM model [50]. For hadronisation and parton showering, PYTHIA 8.212 is used as well, with the AZNLO tune and the CTEQ6L1 PDF set [51].

Different pile-up conditions due to additional pp interactions in the same and neighbouring bunch crossings are simulated by overlaying the hard-scattering event with inelastic pp events generated by PYTHIA8.186 using the NNPDF2.3LO PDF set [52] and the A3 tune [53]. Differences between the simulated and observed distributions of the number of interactions per bunch crossing are corrected by reweighting the simulated events to match the data distribution.

All MC samples use a full simulation of the ATLAS detector [54] based on GEANT [55] to reproduce the detector response. Corrections are applied to the simulated events to match the photon selection efficiencies, energy scale and resolution to those determined in data.

4 Object reconstruction and event selection

The experimental signature of $H \to aa \to 4\gamma$ depends significantly on the ALP mass and on its coupling to photons, $C_{a\gamma\gamma}$. ALP masses below 3.5 GeV dominantly yield collimated photon signatures, which are reconstructed as one energy cluster in the electromagnetic calorimeter. The photons originating from the decays of axion-like particles with higher masses can typically be resolved by the ATLAS calorimeter system and the ATLAS identification algorithms. The $C_{a\gamma\gamma}$ coupling determines the lifetime and hence the distance the ALPs travel after being produced, so the search for $H \to aa \to 4\gamma$ is divided into two sub-searches: a search for promptly decaying ALPs corresponding to couplings $C_{a\gamma\gamma} \geq 0.1$ and a search for long-lived ALPs that is optimised for smaller couplings. Coupling values smaller than $C_{a\gamma\gamma} = 10^{-7}$ cannot be probed within this analysis since they yield ALP lifetimes that imply a decay outside of the detector volume for all ALP masses considered.

4.1 Object reconstruction

Photons are reconstructed from topologically connected clusters [56] of energy deposits in the electromagnetic calorimeter in the region $|\eta| < 2.5$ where a distinction to electrons is provided by the tracking system. Only photon candidates within $|\eta| < 2.37$ are used in this analysis to allow the usage of a track based isolation variable. The transition region between the barrel and endcap electromagnetic calorimeters, $1.37 < |\eta| < 1.52$, is excluded due to poor resolution of the calorimeter in this area. The analysis does not distinguish between photons converting into e^+e^- pairs and unconverted photons.

Photon candidates are defined by the lateral shower profile of the energy deposits in the first and second electromagnetic calorimeter layers and by the fractional energy leakage

into the hadron calorimeter. The analysis uses different photon identification criteria for different regions of the signal parameter space. Standard 'Tight' and 'Loose' photon identification criteria [57,58], which are tuned for converted and unconverted photons separately, are applied in final states where individual photons can be separately reconstructed. Axion-like particles with small masses, e.g., $m_a < 3.5\,\text{GeV}$, decay predominantly into a pair of highly collimated photons, which are reconstructed as single photon object. For these merged photon objects, the standard photon identification is not efficient. Hence, a neural network (NN)-based classification approach is developed. A first classifier is trained to separate real photon signatures, single or collimated, from 'fake photons' that come from multijet background. A second classifier is then trained to separate single-photon signatures from collimated signatures. Both classifiers use eight shower-shape variables relevant for photon identification [58]. The training data sets are based on single- and collimated-photon signatures from simulation and fake-photon candidates from data; the fake-photon candidates are selected by inverting the requirement on several isolation observables. If a photon passes a minimum threshold of the output neurons of both classifiers, it is labelled as a 'merged' photon. The performance of the classifier is shown in Fig. 1. Due to coarse pointing resolution of the calorimeter it is not possible to reconstruct displaced secondary vertices from ALP decays.

The photon energy is reconstructed using the nominal ATLAS reconstruction and calibration procedures [59]. The energy of photon candidates that are identified as collimated photon signatures is corrected by adding the measured cluster energies in the calorimeter within a cone of $\Delta R = 0.2$ around the photon, if not yet associated with the photon.

To further improve the rejection of misidentified photons, a track-based variable $p_{\text{T}}^{\text{iso}}$ is defined as the scalar sum of the transverse momenta of all tracks with transverse momentum (p_{T}) above 1 GeV that originate from the primary vertex and are within a cone of $\Delta R = 0.2$ around the photon candidate with transverse energy E_{T}^{γ}. Isolated photons must have $p_{\text{T}}^{\text{iso}}/E_{\text{T}}^{\gamma} < 0.05$. A calorimeter-based isolation requirement is not used due to its large signal rejection for collimated photon signatures.

4.2 Event selection and categorization

Events are selected using one of two di-photon triggers [60], each of which requires two reconstructed photon candidates. The first trigger requires a minimum transverse energy of 35 GeV for the leading photon and 25 GeV for the subleading photon where both photons must satisfy the online Loose or Medium identification criteria [60], depending on the data-taking period. The alternative trigger requires that each photon satisfy the Tight identification criteria and have a transverse energy of at least 22 GeV. The terms 'leading' and 'subleading' refer to the photon candidate with the highest and second-highest transverse energy, respectively. Photon candidates in the event must have a minimum transverse energy corresponding to the trigger threshold for the leading and subleading photons and at least 15 GeV for any additional photon. For $H \to aa \to 4\gamma$ events with $C_{a\gamma\gamma} = 1$ and at least two selected photon candidates, the average trigger efficiency is larger than 60% for all ALP masses. This still holds for $C_{a\gamma\gamma} = 10^{-5}$ and $m_a > 50\,\text{GeV}$, while for smaller masses the trigger efficiency decreases down to 30 %. The trigger efficiency drops for decreasing ALP masses as collimated photon signatures often fail the isolation requirement at trigger level, which is based on calorimeter information rather than tracks.

Signal events are fully reconstructed if all four photons are detected. However, some of the photons might be out of detector acceptance and some might not be reconstructed. The lifetime of the ALPs depends on their mass and coupling to photons, as shown in Sect. 1. Some examples are listed here: assuming a coupling of $C_{a\gamma\gamma} = 10^{-4}$ a mass of $m_a = 1\,\text{GeV}$ ($m_a = 10\,\text{GeV}$) yields a lifetime of $c\tau = 25\,\text{m}$ ($c\tau = 25\,\text{mm}$). For $C_{a\gamma\gamma} = 10^{-5}$ the lifetime increases by a factor of hundred. Missing photons as well as pairs of collimated photons being reconstructed as one photon result in fewer reconstructed photons. At least two reconstructed photon candidates are required for the analysis. Further classification is based on the number and types of reconstructed photons.

Each event is classified into one of the five categories according to their experimental signature, in the following order: (1) events with four reconstructed photons, where all photons satisfy the Loose identification and at least one satisfies the Tight identification, fall into the four-single (4S) category. (2) events with three reconstructed photons, where all photons satisfy the Tight identification, fall into the three-single (3S) category. (3) events with two merged photon candidates fall into the two-merged (2M) category. Additional loose photon candidates are likely to originate from background processes and are ignored, with negligible impact on the rate of falsely identified signal events. (4) events with two photon candidates, where one satisfies the merged classification and the other satisfies the Loose identification, fall into the one-merged-one-single (1M1S) category. This category accepts events where the merged classification of two photons is not efficient. (5) events with exactly two photons that satisfy the Tight identification but without any further photon candidates that satisfy the Loose identification fall into the two-single category (2S), which is dominated by events from the $H \to \gamma\gamma$ process.

Only the most sensitive categories are used for the ALP search. For long-lived ALPs with masses $m_a \geq 3.5\,\text{GeV}$ the 3S and 4S categories provide the most sensitivity. Long-lived ALPs with $m_a < 3.5\,\text{GeV}$ yield collimated photon

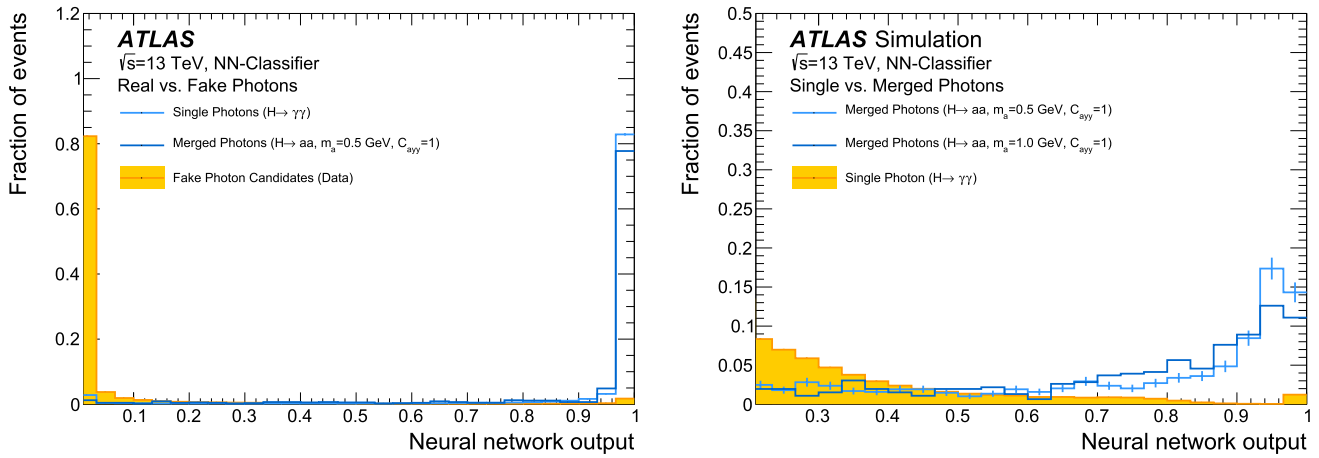

(a) (b)

Fig. 1 Output of the neural network classifier to distinguish **a** real from fake photons, and **b** single from merged photons

signatures where the 2M, and 1M1S categories provide the largest sensitivity.

The 3S and 4S categories allow for the reconstruction of the ALP mass, m_a, since at least one photon pair stems from the decay of an ALP for the signal process. Separate neural networks were trained for the three- and four-photon categories to select the correct photon pairing(s). The inputs to the networks are the invariant masses of all photon pair combinations and differences in their transverse energies and directions. The training sample consists of both correct and wrong photon combinations. The combinations are based on MC signal samples for all ALP masses and couplings. In the 3S category, the invariant mass of the photon pair that is predicted to stem from the same mother particle is defined as the reconstructed ALP mass m_a^{reco}, while the average of both resulting invariant masses is defined as m_a^{reco} in the 4S category.

The signal region selection uses the invariant mass of all photon candidates, denoted by $m_{\text{inv}}^{\text{reco}}$, which is expected to peak around the Higgs boson mass for signal processes. The signal regions for all categories and searches are defined to contain at least 90% of the reconstructed signal contribution in simulated data. For the two-photon categories (2M, 1M1S and 2S), the signal region is defined by the invariant mass requirement $115\,\text{GeV} < m_{\text{inv}}^{\text{reco}} < 130\,\text{GeV}$ around the Higgs boson mass.

The 3S and 4S categories also require the reconstructed ALP mass m_a^{reco} to fall within a window around the generated ALP mass, whose size varies depending on the mass point being tested. In general, the requirements on $m_{\text{inv}}^{\text{reco}}$ are looser in the 3S category since one photon typically escapes detection, leading to a wider $m_{\text{inv}}^{\text{reco}}$ spectrum. The m_a^{reco} distribution also enables the definition of a control region in data by inverting the mass requirement on m_a^{reco}.

In the search for promptly decaying ALPs only the 4S category is used when estimating the limits on the signal process, as it has by far the largest sensitivity. In this case the category is defined by tightening the selection cuts so that at least three out of the four photons satisfy the Tight identification requirements and is labelled $4S_p$. Promptly decaying ALPs are only considered for $m_a > 5$ GeV, where a significant increase in sensitivity over the search for long-lived ALPs is observed. Table 1 summarizes the signal region definitions for all ALP mass hypotheses m_a.

5 Background estimation

The main background contributions stem from multijet processes, where jets might be misidentified as photons, as well as Standard Model multiphoton processes. However, as the simulation does not capture the full background shape observed in data we rely on a fully data driven background estimate.

The signal is expected to peak in $m_{\text{inv}}^{\text{reco}}$, the invariant mass of the selected photons, near the Higgs boson mass, $m_H = 125$ GeV, in all categories and searches. The $m_{\text{inv}}^{\text{reco}}$ sidebands are used for the background estimate in the signal region and for the estimation of spurious signal effects.

5.1 Two-photon final states in the search for long-lived axion-like particles

The distribution of $m_{\text{inv}}^{\text{reco}}$ in all two-photon categories (2M, 1M1S, 2S) is fitted over a mass range from 100 to 150 GeV, region excluding the signal region. A suitable fitting function should describe the data in the sidebands, provide an unbiased estimate of the background in the signal region, and

Table 1 Definition of the signal region for different event categories in the prompt and long-lived search

Model parameters	Signal region definition	
Long-lived ALP search: $C_{a\gamma\gamma} < 0.1$		
	2M, 1M1S and 2S categories	
$0.1\ \text{GeV} \leq m_a < 3.5\ \text{GeV}$	$115\ \text{GeV} < m_{\text{inv}}^{\text{reco}} < 130\ \text{GeV}$	
	3S category	4S category
$3.5\ \text{GeV} \leq m_a < 10\ \text{GeV}$	$105\ \text{GeV} < m_{\text{inv}}^{\text{reco}} < 130\ \text{GeV}$	$120\ \text{GeV} < m_{\text{inv}}^{\text{reco}} < 130\ \text{GeV}$
	$0\ \text{GeV} < m_a^{\text{reco}} < 10\ \text{GeV}$	$0\ \text{GeV} < m_a^{\text{reco}} < 12\ \text{GeV}$
$10\ \text{GeV} \leq m_a < 25\ \text{GeV}$	$100\ \text{GeV} < m_{\text{inv}}^{\text{reco}} < 125\ \text{GeV}$	$120\ \text{GeV} < m_{\text{inv}}^{\text{reco}} < 130\ \text{GeV}$
	$6\ \text{GeV} < m_a^{\text{reco}} < 26\ \text{GeV}$	$8\ \text{GeV} < m_a^{\text{reco}} < 28\ \text{GeV}$
$25\ \text{GeV} \leq m_a < 40\ \text{GeV}$	$100\ \text{GeV} < m_{\text{inv}}^{\text{reco}} < 125\ \text{GeV}$	$120\ \text{GeV} < m_{\text{inv}}^{\text{reco}} < 130\ \text{GeV}$
	$20\ \text{GeV} < m_a^{\text{reco}} < 40\ \text{GeV}$	$23\ \text{GeV} < m_a^{\text{reco}} < 43\ \text{GeV}$
$40\ \text{GeV} \leq m_a \leq 62\ \text{GeV}$	$90\ \text{GeV} < m_{\text{inv}}^{\text{reco}} < 115\ \text{GeV}$	$120\ \text{GeV} < m_{\text{inv}}^{\text{reco}} < 130\ \text{GeV}$
	$30\ \text{GeV} < m_a^{\text{reco}} < 65\ \text{GeV}$	$38\ \text{GeV} < m_a^{\text{reco}} < 65\ \text{GeV}$
Prompt ALP search: $0.1 < C_{a\gamma\gamma} < 1$		
		$4S_p$ category
$5\ \text{GeV} \leq m_a < 25\ \text{GeV}$		$120\ \text{GeV} < m_{\text{inv}}^{\text{reco}} < 130\ \text{GeV}$
		$\lvert m_a - m_a^{\text{reco}} \rvert < 1\ \text{GeV}$
$25\ \text{GeV} \leq m_a < 40\ \text{GeV}$		$120\ \text{GeV} < m_{\text{inv}}^{\text{reco}} < 130\ \text{GeV}$
		$\lvert m_a - m_a^{\text{reco}} \rvert < 2\ \text{GeV}$
$40\ \text{GeV} \leq m_a < 50\ \text{GeV}$		$120\ \text{GeV} < m_{\text{inv}}^{\text{reco}} < 130\ \text{GeV}$
		$\lvert m_a - m_a^{\text{reco}} \rvert < 3\ \text{GeV}$
$50\ \text{GeV} \leq m_a < 55\ \text{GeV}$		$120\ \text{GeV} < m_{\text{inv}}^{\text{reco}} < 130\ \text{GeV}$
		$\lvert m_a - m_a^{\text{reco}} \rvert < 5\ \text{GeV}$
$55\ \text{GeV} \leq m_a \leq 62\ \text{GeV}$		$120\ \text{GeV} < m_{\text{inv}}^{\text{reco}} < 130\ \text{GeV}$
		$\lvert m_a - m_a^{\text{reco}} \rvert < 8\ \text{GeV}$

produce small uncertainties on the yields of spurious signals. This is ensured by defining validation regions that use similar requirements to those of the signal region but reject signal events. Simulated samples of two-photon continuum processes and a data-driven validation region are studied. The latter is defined using the nominal signal selection and classification, but inverting the isolation cut on the photon candidates, thus yielding a multijet-enhanced data sample.[2] These validation regions are chosen to cover any scenario between a background composed purely of di-photon events and a background consisting of mis-identified multijet events.

A Landau function gives unbiased background estimates in the signal region of both validation samples and provides χ^2 per number of degrees of freedom around unity ($\chi^2/\text{ndf} \approx 1$) in all sideband regions for the 2S and 1M1S categories. It is expected that the background shape in the 2M category differs from the 2S and 1M1S categories, due to the different background composition after the requirements on the NN-based classifiers. A second-order polynomial provides a good description of all validation regions of the 2M category. Variations of the background estimates using different fitting functions and different fitting ranges are used to define systematic uncertainties and are discussed in Sect. 6.

The $H \to \gamma\gamma$ process contributes not in the sideband but in the signal region as irreducible background, significantly in the 2S category and to a negligible extent in the 2M and 1M1S categories. Its contribution and shape are estimated by MC predictions.

Figure 2 shows the $m_{\text{inv}}^{\text{reco}}$ spectra including the sideband fit for the signal selection for the 2M and 1M1S categories, respectively. The expected signal shape for an ALP with $m_a = 0.5\,\text{GeV}$ and $C_{a\gamma\gamma} = 0.01$ is also shown for illustration.

5.2 Three- and four-photon final states in the search for long-lived axion-like particles

The background estimation in the long-lived ALPs searches also employs a sideband fit using the $m_{\text{inv}}^{\text{reco}}$ spectrum in the 3S and 4S categories.

[2] It is ensured that there is no overlap with the training data of the NN-based photon identification classifiers.

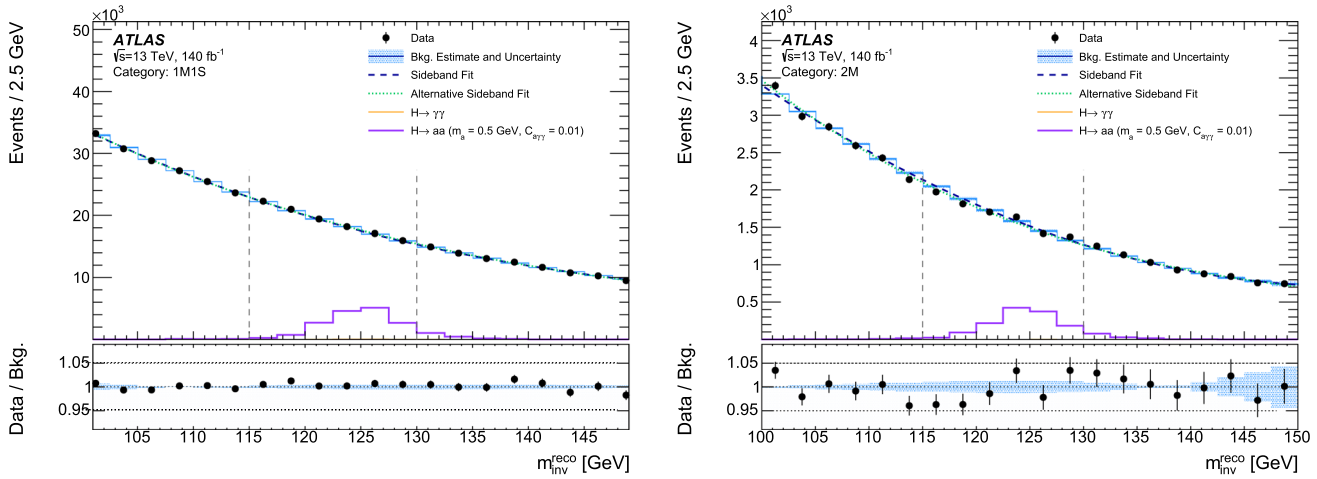

(a) (b)

Fig. 2 $m_{\text{inv}}^{\text{reco}}$ distribution for the nominal signal selection for the **a** 1M1S and **b** 2M category. The nominal sideband fitting function is shown as the blue dashed line. The background, estimated from a fit in the side-band regions, and its systematic uncertainty is shown as a blue histogram for both cases. The green dotted line shows the alternative fitting function used to estimate the spurious signal uncertainty (discussed in Sect. 6). The expected signal shape for $m_a = 0.5\,\text{GeV}$, $C_{ayy} = 0.01$ is also shown with an arbitrary normalization. The signal region selection on $m_{\text{inv}}^{\text{reco}}$ is indicated using vertical dashed lines. The contribution from $H \to \gamma\gamma$ is negligible and not visible in the figures. The lower panels show the data divided by the estimated continuum background, where the shaded area indicates the uncertainty on the background estimation

Polynomials of third and second order serve as the nominal background fitting functions for the 3S and 4S categories, respectively, where the fits are carried out in the range of 80–150 GeV and 105–145 GeV, excluding the signal region. First, the suitability of the sideband functions for background estimation in both categories is tested on three- and four-photon continuum MC samples. Next, the sideband functions and corresponding background estimates are validated using an orthogonal set of data events in which the requirement on the reconstructed ALP mass is inverted.

This inverted sample can be used as a validation region, since the shape of background events should not change with a different choice of ALP mass apart from minor kinematic changes in the $m_{\text{inv}}^{\text{reco}}$ distribution. The multi-photon MC samples are used to correct for this kinematic effect.

The chosen fitting functions yield a χ^2/ndf close to unity in all validation regions and the estimated background using these validation regions is consistent with the observed numbers of background events from the signal region sidebands. Systematic uncertainties due to the choice of the background function and the fitting range are discussed in Sect. 6. Figure 3 depicts the $m_{\text{inv}}^{\text{reco}}$ spectrum for various ALP mass searches, and shows the sideband fitting functions, the estimated background in the signal region, and the expected signal shape for two $C_{a\gamma\gamma}$ coupling parameters.

5.3 Four-photon final states in the search for promptly decaying axion-like particles

The number of selected events in the $4S_p$ category of the search for promptly decaying ALPs, also defined in the $m_{\text{inv}}^{\text{reco}}$ vs. m_a^{reco} plane, is significantly lower than that in the analysis optimised for long-lived ALPs due to the stricter rejection of fake-photon signatures using more stringent selection criteria such as Tight photon identification. To further suppress background contributions in the signal region, a tight selection around the m_a model parameter, as discussed in Sect. 4, is imposed. The size of the signal regions for each ALP mass are shown in Table 1. The background in the signal region of the search for promptly decaying ALPs is estimated by counting the events around the signal region in the $m_{\text{inv}}^{\text{reco}}$-$m_a^{\text{reco}}$ plane, extending the signal region by $\pm 5\,\text{GeV}$ in the $m_{\text{inv}}^{\text{reco}}$ dimension and by 1.5 times the signal region width in the m_a^{reco} dimension. Due to the low statistics, the total number of background events in the shaded sideband area is scaled by the ratio of the areas of the signal region to the sideband region to estimate the number of background events in the signal region, as illustrated in Fig 4. This is equivalent to assuming a flat background distribution in the plane.

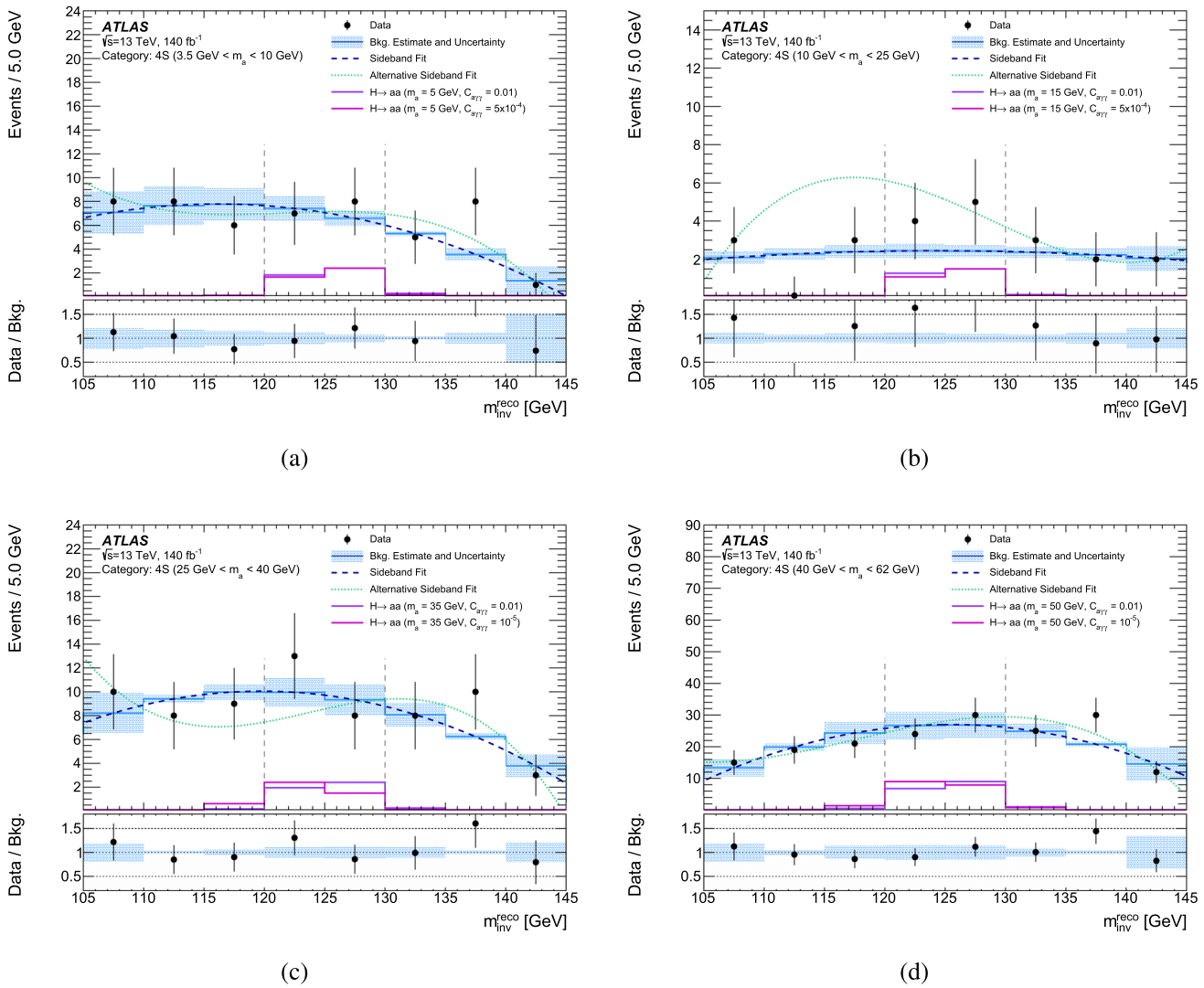

Fig. 3 $m_{\text{inv}}^{\text{reco}}$ distribution for the nominal signal selection for the 4S category. The nominal sideband fitting function is shown as the blue dashed line. The background, estimated from a fit in the side-band regions, and its systematic variation (obtained from a fit with reduced range) is shown as the blue histogram. The green dotted line shows the alternative fitting function which is used to estimate the spurious signal uncertainty (discussed in Sect. 6). The four subfigures show different ALP mass ranges: **a** $3.5\,\text{GeV} < m_a < 10\,\text{GeV}$, **b** $10\,\text{GeV} < m_a < 25\,\text{GeV}$, **c** $25\,\text{GeV} < m_a < 40\,\text{GeV}$, **d** $40\,\text{GeV} < m_a < 62\,\text{GeV}$. The signal region selection on m_a^{reco} is applied while the signal region selection on $m_{\text{inv}}^{\text{reco}}$ is indicated as dashed lines. The expected signal shapes for $m_a = 5\,\text{GeV}, C_{ayy} = 0.01$; $m_a = 5\,\text{GeV}, C_{ayy} = 5 \cdot 10^{-4}$; $m_a = 15\,\text{GeV}, C_{ayy} = 0.01$; $m_a = 15\,\text{GeV}, C_{ayy} = 5 \cdot 10^{-4}$; $m_a = 35\,\text{GeV}, C_{ayy} = 0.01$; $m_a = 35\,\text{GeV}, C_{ayy} = 10^{-5}$; $m_a = 50\,\text{GeV}, C_{ayy} = 0.01$; $m_a = 50\,\text{GeV}, C_{ayy} = 10^{-5}$;is shown with arbitrary normalization. The lower panels show the data divided by the estimated continuum background, where the shaded area indicates the uncertainty on the background estimation

As an alternative background estimate, the size of the control region is taken to be 2.5 times the signal region instead of the 1.5 times used in the nominal background estimate. The difference between the nominal and the alternative background estimates is used as a systematic uncertainty. Figure 4 shows distributions in the $m_{\text{inv}}^{\text{reco}}$-$m_a^{\text{reco}}$ plane for events selected in the search for promptly decaying ALPs, with the sideband regions shown for the search parameters $m_a = 10$ GeV and $m_a = 40$ GeV. The validity of this procedure was tested using simulated multi-photon samples confirming that the associated statistical and systematic uncertainties cover potential shape differences.

5.4 Background estimate summary

Table 2 summarizes the data and the expected background contribution in the signal region for the different categories. The acceptance times selection efficiency of a signal event in any of the categories is largely dependent on the ALP mass and coupling parameters under investigation. It ranges from

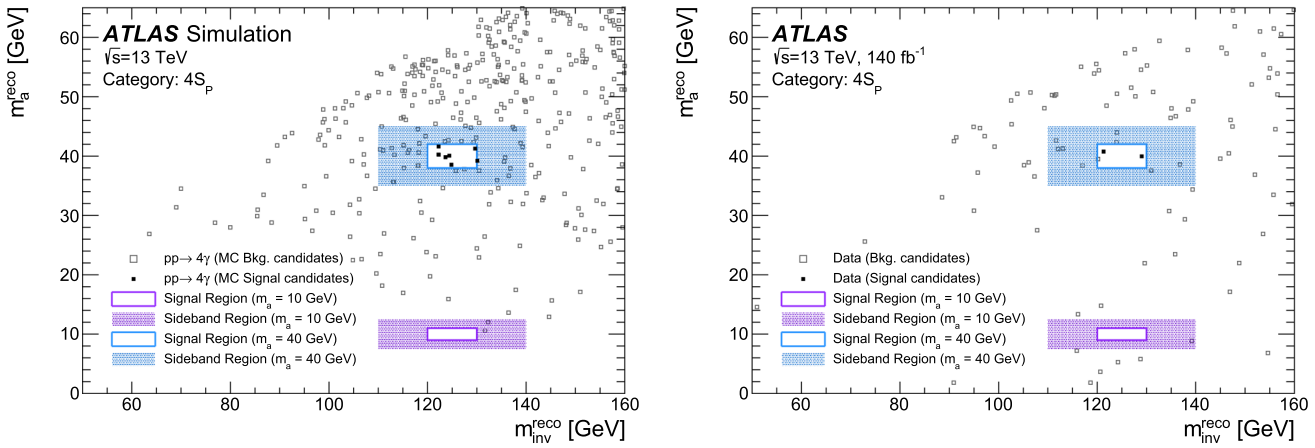

(a) (b)

Fig. 4 $m_{\text{inv}}^{\text{reco}}$ vs. m_a^{reco} for the $4S_p$ categories in the search for promptly decaying ALPs, for **a** simulated $pp \to 4\gamma$ sample and **b** for data. The signal (sideband) regions are indicated by solid lines (shaded areas) for the searches for ALPs with masses of 10 GeV and 40 GeV. Events within the signal region are shown with filled markers, those outside with open markers

9 to 23% for low ALP masses ($m_a < 5$ GeV) and large couplings ($C_{a\gamma\gamma} = 1$) and is around 13% for large ALP masses ($m_a \approx 60$ GeV) at all studied couplings. The largest fraction of events are already cut by the trigger due to the relatively high trigger thresholds. A future reduction of the trigger thresholds could significantly improve the analysis acceptance.

6 Systematic uncertainties

The systematic uncertainties are assessed below, and their impact on the results is discussed in Sect. 7. First the general experimental uncertainties are discussed, where special attention is given to the uncertainties arising from the displaced decay of long lived ALPs. Then the uncertainties impacting the background estimation are detailed followed by a discussion of the relevant theoretical uncertainties.

The experimental systematic uncertainty ranges, depending on the category and the hypothesized ALP mass and coupling, from 6.5% to 18% for most categories, with the exception of the 4S category where the uncertainty rises to 40% for masses $m_a < 15$ GeV and small couplings $C_{a\gamma\gamma}$ due to low statistics and large contributions from the photon identification uncertainties. The theoretical uncertainty is around 6% for all categories.

6.1 General experimental uncertainties

The following general experimental systematics are applied to the signal model.

The uncertainty in the combined 2015–2018 integrated luminosity is 0.83% [35], obtained using the LUCID-2 detector [61] for the primary luminosity measurements, complemented by measurements using the inner detector and calorimeters.

To evaluate any impact on the expected signal yield due to imperfect modelling of pile-up, the average number of pile-up interactions is varied in the simulation. The corresponding uncertainty is below 1%.

The trigger efficiency used to select events is evaluated in simulation and data using a bootstrap method and radiative Z-boson decays [60]. The difference between data and simulation, which ranges from 2 to 3%, is taken as a systematic uncertainty.

The systematic uncertainties from the standard photon identification and isolation efficiencies are estimated following the prescriptions in Ref. [58]. They affect the di-photon selection efficiency and are evaluated by varying the correction factors for photon selection efficiencies in simulation by their corresponding uncertainties. The experimental uncertainties in the photon energy scale and resolution are obtained as described in Ref. [58]. These variations produce uncertainties below 3% on the expected number of events in the signal region in the search for promptly decaying ALPs.

The uncertainties of the NN-based classifiers are estimated by comparing their identification performance using $Z \to ee$ events in simulation and data, where the electron shower-shape variables are used as the network input variables. Very good agreement of the network output between data and simulation is observed. The residual differences are fully propagated as uncertainties on the expected signal yields and pro-

Table 2 Overview of the number of observed events in the search for long-lived ALPs (left) and selected mass points from the search for prompt ALPs (right) in comparison to the expected number of background events. The uncertainty on the background estimate includes statistical and systematic uncertainties as described in Sect. 6

Long-lived ALP search			Prompt ALP search		
Category $C_{a\gamma\gamma} < 0.1$	Events	Background estimate	Category $0.1 < C_{a\gamma\gamma} < 1$	Events	Background estimate
2M	9917	$10{,}000 \pm 200$	$4\mathrm{S}_p$ ($m_a = 5$ GeV)	2	0.35 ± 0.27
1M1S	113,875	$113{,}100 \pm 700$	$4\mathrm{S}_p$ ($m_a = 10$ GeV)	0	0.24 ± 0.18
2S	632,484	$634{,}000 \pm 1500$	$4\mathrm{S}_p$ ($m_a = 15$ GeV)	1	0.24 ± 0.28
3S ($3.5\,\mathrm{GeV} \leq m_a < 10\,\mathrm{GeV}$)	4782	4800 ± 100	$4\mathrm{S}_p$ ($m_a = 20$ GeV)	0	0.24 ± 0.28
3S ($10\,\mathrm{GeV} \leq m_a < 25\,\mathrm{GeV}$)	3166	3200 ± 100	$4\mathrm{S}_p$ ($m_a = 25$ GeV)	0	0.24 ± 0.28
3S ($25\,\mathrm{GeV} \leq m_a < 40\,\mathrm{GeV}$)	3843	3900 ± 150	$4\mathrm{S}_p$ ($m_a = 30$ GeV)	0	0.60 ± 0.27
3S ($40\,\mathrm{GeV} \leq m_a \leq 62\,\mathrm{GeV}$)	5389	5600 ± 90	$4\mathrm{S}_p$ ($m_a = 35$ GeV)	0	1.31 ± 0.76
4S ($3.5\,\mathrm{GeV} \leq m_a < 10\,\mathrm{GeV}$)	15	14 ± 3	$4\mathrm{S}_p$ ($m_a = 40$ GeV)	2	1.55 ± 0.94
4S ($10\,\mathrm{GeV} \leq m_a < 25\,\mathrm{GeV}$)	9	4 ± 2	$4\mathrm{S}_p$ ($m_a = 45$ GeV)	2	3.23 ± 0.95
4S ($25\,\mathrm{GeV} \leq m_a < 40\,\mathrm{GeV}$)	21	19 ± 3	$4\mathrm{S}_p$ ($m_a = 55$ GeV)	7	2.84 ± 1.51
4S ($40\,\mathrm{GeV} \leq m_a \leq 62\,\mathrm{GeV}$)	54	54 ± 6	$4\mathrm{S}_p$ ($m_a = 62$ GeV)	4	4.52 ± 1.50

duce normalisation uncertainties of up to 15% in the 2M and 1M1S categories, respectively.

6.1.1 Uncertainties due to displaced ALP decays

The uncertainties related to photon identification and energy reconstruction for photons produced with displaced vertices – i.e., those arising from long-lived ALP decays – are estimated by studying the decays of long-lived hadrons, mainly kaons with transverse momentum $p_{\mathrm{T}} > 10\,\mathrm{GeV}$, which can be reconstructed as displaced tracks in the ATLAS tracking system. The daughter tracks from these decays, which originate from a displaced vertex, can be matched to reconstructed clusters in the electromagnetic calorimeter. A comparison of the shower shapes predicted by simulations to those from data for signatures with displaced vertices can then be used to estimate systematic uncertainties in photon reconstruction. The MC prediction of the shower shapes of hadronic particles also relies on the correct description of particle multiplicities and energies. To correct for any mismatch of particle composition in data and simulation, scale factors are derived from the differences between data and MC predictions for shower-shape variables of tracks close to the primary vertex ($z_0 < 20$ mm and $d_0 < 1$ mm, where z_0 and d_0 are the longitudinal distance from the IP and the impact parameter, respectively). These deviations are taken as a nominal bias and are used to correct tracks originating from a distance between $20\,\mathrm{mm} < z_0 < 500\,\mathrm{mm}$ and $1\,\mathrm{mm} < d_0 < 80\,\mathrm{mm}$ from the primary vertex (medium regime), and tracks with an origin further than $z_0 > 500$ mm and $d_0 > 80$ mm from the interaction point (far regime). These systematic uncertainties are used additionally for all photons stemming from a displaced decay. The systematic uncertainty from the modelling of the NN classifier that discriminates real photons from fakes due to displaced photon vertices is 3%. The corresponding uncertainties from the modelling of the photon identification and the second NN, which discriminates between merged and resolved photons, ranges from 4 to 23%, depending on the displacement.

Long-lived hadrons are also utilized to estimate systematic uncertainties in energy reconstruction. The observed differences in the momentum over energy ratio between the prompt, medium and far regimes are found to be negligible compared to the nominal energy reconstruction uncertainty.

Systematic uncertainties in identifying the correct ALP pairing are mainly caused by variations in the photon energy scale corrections within their uncertainties. The final impact on the number of reconstructed events in a particular ALP mass signal region is less than 5% and hence negligible.

6.2 Uncertainties on the background estimation

The continuum background processes are estimated from data and are subject to uncertainties related to the potential bias arising from the selected background model, as detailed in Sect. 5. The nominal background estimate in each bin is calculated using the nominal fitting functions, which have been fitted in the sideband regions. The shape uncertainty of the background is estimated by employing the same nominal fitting functions, but fitting them in a sideband region whose width is varied by 5 GeV, corresponding to a 25% to 100% change in the fit range, depending on the category, allowing for a large variability of the background shape. The spurious signal bias or background model bias is assessed as an additional uncertainty on the total number of signal events in each category. This bias is estimated by generating pseudo-

data using a modified background model and performing the full signal-plus-background fit (see Sect. 7) on these pseudo-data [62]. The alternative background model for the spurious signal bias estimate is based on a second-order polynomial for the 2M, 1M1S, 3S, and 4S categories, while the function $f_{\text{sys}} = N_0 \exp(p \cdot x) + N_1 + a \cdot x^2 + b \cdot x$ is used for the 2S category. The estimated signal-strength in these pseudo-data is considered as an additional systematic uncertainty in the final signal-strength estimation. The largest impact is found in the 4S category shifting the branching ratio limit by 10^{-6}.

6.3 Impact of theory uncertainties

To estimate the effects of scale uncertainties arising from missing higher-order corrections in the theoretical calculations, the factorisation and renormalisation scales are varied up and down by a factor of two from their nominal values. The cross-section is then recalculated for each case, and the largest deviation from the nominal cross-section is taken as the uncertainty. The uncertainties on the SM Higgs ggF production cross-section due to the choice of renormalisation scheme and top-quark mass, as well as their combination with those from factorisation and renormalisation scale variations, are based on Ref. [63]. The uncertainties in the cross-sections, which include the effects of uncertainties on the PDF and the strong coupling constant α_s, and the uncertainties in the $H \to \gamma\gamma$ branching fractions, are taken from Ref. [46] to be 5.7%. It is found that further uncertainties on the Higgs boson signal prediction are negligible.

The uncertainties on the Higgs boson production cross-section enter when calculating the limit on the branching ratio of the signal process on all Higgs boson decays. The values for the uncertainties are taken from Ref. [46].

7 Results

The statistical analysis is carried out using the PyHF framework [64,65]. In the long-lived ALP searches, the analysis results are obtained by performing a simultaneous maximum-likelihood fit to the $m_{\text{inv}}^{\text{reco}}$ distribution over the range 100 GeV to 150 GeV for the two most sensitive categories for each ALP mass and coupling parameter. The 2M and 1S1M categories are most sensitive for low ALP masses ($m_a < 5$ GeV), while for larger ALP masses, the 4S category dominates over the 3S category. Including more than two categories in the fit does not significantly improve the sensitivity for any model parameter. In the prompt ALP search, only the number of events in the signal region of the $4S_p$ category is used. The analysis sensitivity is limited by the available data statistics for the $4S$ and $4S_p$ categories, while the systematic uncertainties dominate in other categories. The likelihood function is defined as follows:

$$\mathcal{L} = \prod_c \left(\text{Pois}(n_c | N_c(\boldsymbol{\theta})) \cdot \prod_{i=1}^{n_{\text{bins}}^c} f_c(n_i, m_{\text{inv}}^{\text{reco},i}, \boldsymbol{\theta}) \right) \cdot G(\boldsymbol{\theta}). \tag{1}$$

Here, n_{bins}^c is the number of bins in the $m_{\text{inv}}^{\text{reco}}$ distribution, n_c is the observed number of events, and N_c is the expected number of events for each category c. For each bin i in the $m_{\text{inv}}^{\text{reco}}$ distribution of category c, f_c is the value of the probability density function (pdf) which is estimated from simulation, n_i is the number of observed events in bin i, $\boldsymbol{\theta}$ represents the nuisance parameters (NP) used to parametrize the effect of systematic uncertainties, and $G(\boldsymbol{\theta})$ represents constraint pdfs for the nuisance parameters. All constraints correspond to Gaussian pdfs. The expected number of events N_c is defined as the sum of the expected yields from $H \to aa \to 4\gamma$ production processes ($N_{H\to aa}$), single Higgs-boson production ($N_{\text{bkg}}^{\text{H}\to\gamma\gamma}$), the non-resonant background ($N_{\text{bkg,c}}^{\text{nonres}}$), and the spurious signal uncertainty ($N_{\text{SS,c}}$). It is defined as:

$$\begin{aligned} N_c(\boldsymbol{\theta}) = \mu \cdot N_{H\to aa}(\boldsymbol{\theta}_{H\to aa}^{\text{yield}}) + N_{\text{bkg}}^{\text{H}\to\gamma\gamma}(\boldsymbol{\theta}_{\text{H}\to\gamma\gamma}^{\text{yield}}) \\ + N_{\text{bkg,c}}^{\text{nonres}}(\boldsymbol{\theta}_{\text{nonres}}^{\text{yield}}) + N_{\text{SS,c}}. \end{aligned} \tag{2}$$

Here, μ is the signal strength, and $\boldsymbol{\theta}^{\text{yield}}$ represents the NPs affecting the event yield, as described in Sect. 6. Correlation of the nuisance parameters across different signal and background components, and categories, is taken into account. The normalisation parameter for the $H \to \gamma\gamma$ production rate, $\boldsymbol{\theta}_{\text{H}\to\gamma\gamma}^{\text{yield}}$, is set to 1 and corresponds to the SM prediction for the $H \to \gamma\gamma$ cross-section. It is allowed to vary within its theoretical and experimental uncertainties.

The signal-plus-background hypothesis for the production of a Higgs boson that decays into ALPs is tested using the profile-likelihood-ratio test statistic derived from Eq. 1, and is parameterized with the signal-strength parameter μ. This parameter is defined as the ratio of the extracted signal events to the total number of signal events in the MC simulation.[3]

Figure 5 shows the distribution of the number of estimated and observed events in the signal region of the most sensitive category for various ALP masses and coupling parameters for the prompt and long-lived ALP searches. Good agreement is observed between the estimated backgrounds and the data. No significant pulls of the NP are observed after the fits. The NP $\boldsymbol{\theta}_{\text{H}\to\gamma\gamma}^{\text{yield}}$ is found to be consistent with 1, corresponding to the expected SM Higgs boson production cross-section on the 2S category.

Upper limits, derived using the CLs technique [66], are set on $\mathcal{B}(H \to aa \to 4\gamma)$. The branching ratio is obtained

[3] Only $H \to aa \to 4\gamma$ events are simulated in the signal samples, i.e., the branching ratio for this process is unity in the simulation.

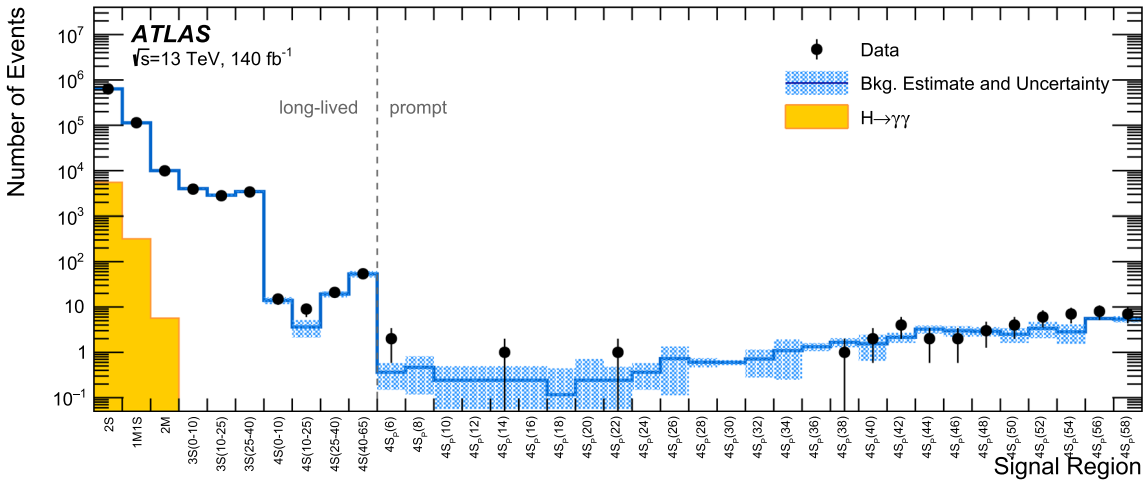

Fig. 5 The number of data and estimated background events in the signal region of the most sensitive categories. The uncertainty in the background estimate is shown as shaded band. The left side shows the different categories of the long-lived ALP search, while the right side displays the $4S_p$ category of the prompt search for increasing mass hypotheses. The numbers in parentheses in the x-axis labels correspond to the probed ALP mass hypothesis in GeV. The SM $H \to \gamma\gamma$ background is only sizeable in the first three bins, corresponding to the two-photon categories

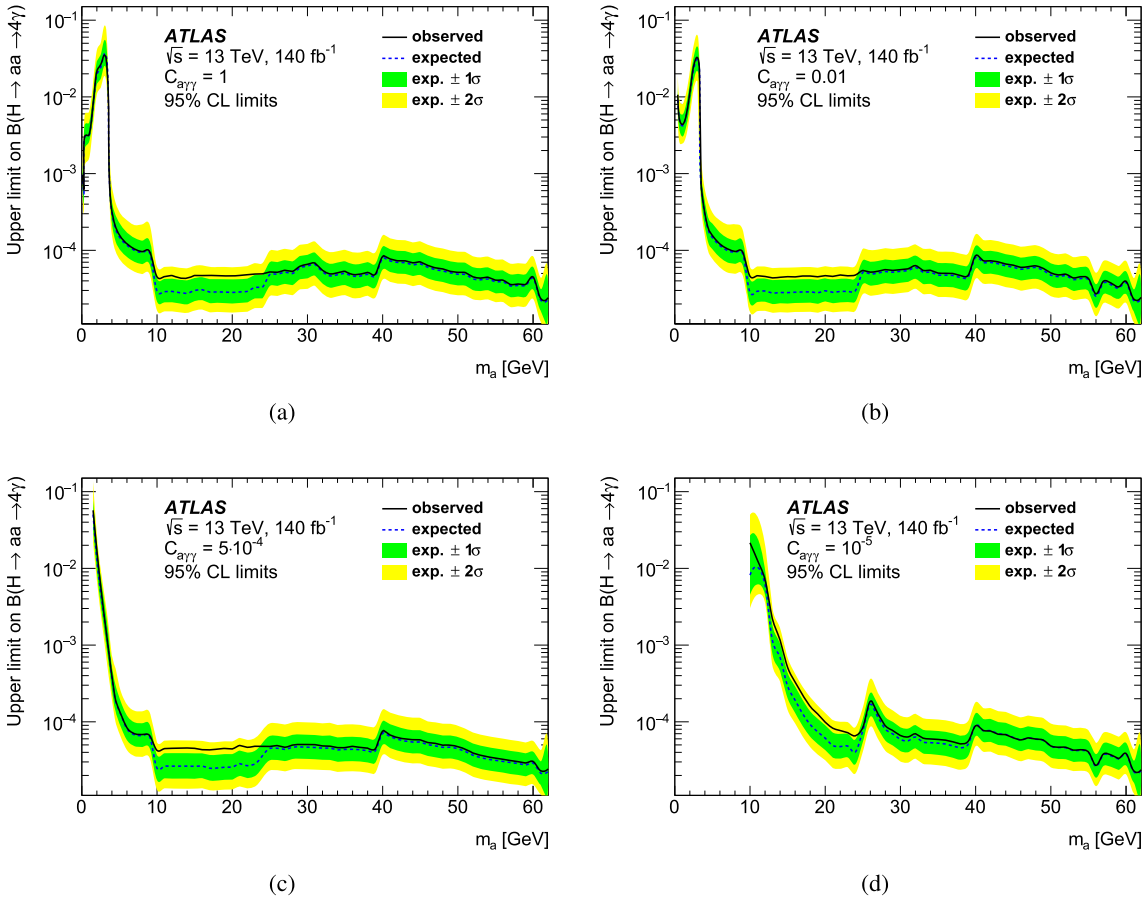

Fig. 6 Upper limits on $\mathcal{B}(H \to aa \to 4\gamma)$ at 95% CL as a function of the axion mass and for different ALP-photon couplings, from **a** $C_{a\gamma\gamma} = 1$ to **d** $C_{a\gamma\gamma} = 10^{-5}$

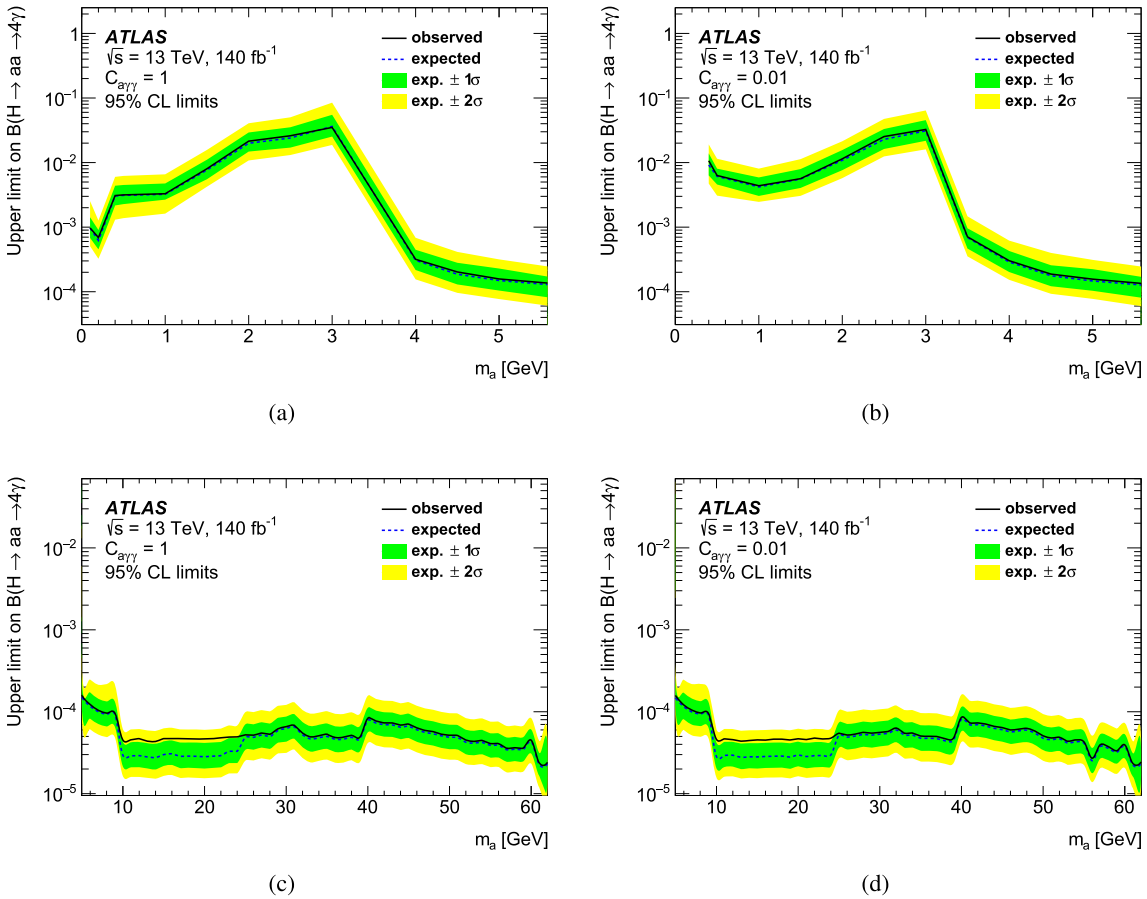

Fig. 7 Zoomed in version of Fig. 6 showing upper limits on $\mathcal{B}(H \to aa \to 4\gamma)$ at 95% CL as a function of the signal mass hypothesis and for different ALP-photon couplings. **a** $m_a < 5.0\,\text{GeV}$, $C_{a\gamma\gamma} = 1$; **b** $m_a < 5.0\,\text{GeV}$, $C_{a\gamma\gamma} = 0.01$; **c** $m_a > 5.0\,\text{GeV}$, $C_{a\gamma\gamma} = 1$; **d** $m_a > 5.0\,\text{GeV}$, $C_{a\gamma\gamma} = 0.01$

by dividing the fitted signal cross-section by the total Higgs-boson production cross-section of 55.6 pb [46]. The expected and observed limits as a function of m_a from the search optimized for long-lived ALPs, i.e., $C_{a\gamma\gamma} < 0.1$, are shown in Fig. 6 along with the performance on prompt decays for $C_{a\gamma\gamma} = 1$. For low masses and low couplings, the lifetime of the ALP gets significantly larger and most of the ALPs decay outside the active detector area. Therefore there are no limits available for $C_{a\gamma\gamma} \leq 5 \times 10^{-4}$ and $m_a < 10$ GeV. Limits for prompt decays with $C_{a\gamma\gamma} = 1$ are also shown. A relatively uniform sensitivity is achieved for larger ALP masses, above 10 GeV for $C_{a\gamma\gamma} \geq 5 \times 10^{-4}$ and above 25 GeV for $C_{a\gamma\gamma} = 10^{-5}$. The sensitivity for low ALP masses decreases with smaller coupling values, as more ALP decays happen outside the sensitive detector volume. The largest differences between expected and observed limits are found in long-lived ALP searches for masses between 10 and 25 GeV at 1.5 σ. It should be noted that the background estimation is the same for all couplings in this mass region. Hence correlated behaviour is expected for all relevant couplings. The limits for the couplings $C_{a\gamma\gamma} = 1$ and $C_{a\gamma\gamma} = 0.01$ as a function of m_a are shown in Fig. 7, separated for low ALP masses ($m_a < 5\,\text{GeV}$) and higher ALP masses. The upper limits at 95% CL on $\mathcal{B}(H \to aa \to 4\gamma)$ range from 10^{-4} to 3×10^{-2} for low ALP masses and from 2×10^{-5} to 2×10^{-4} for higher ALP masses. The observed limits are compatible with the expected limits. The loss in sensitivity around 3 GeV is due to the transition between the merged and resolved photon categories, where the former have significantly larger background contributions.

The limits on $\mathcal{B}(H \to aa \to 4\gamma)$ derived from the $4S_p$ category assuming promptly decaying ALPs are shown in Fig. 8. The derived limit is mostly flat at $\mathcal{B} < 2 \times 10^{-5}$ in the mass range $10\,\text{GeV} < m_a < 62\,\text{GeV}$. For the long-lived searches it is necessary to loosen the selection criteria to allow for displaced ALP decays. Therefore the background contributions are significantly larger and consequently the searches are less sensitive than the prompt searches. The observed limits are consistent with the expected limits.

The limits on ALP masses with $m_a > 15$ GeV are about one order of magnitude more stringent than previous ATLAS analyses [26] using 8 TeV data, and reach similar to slightly

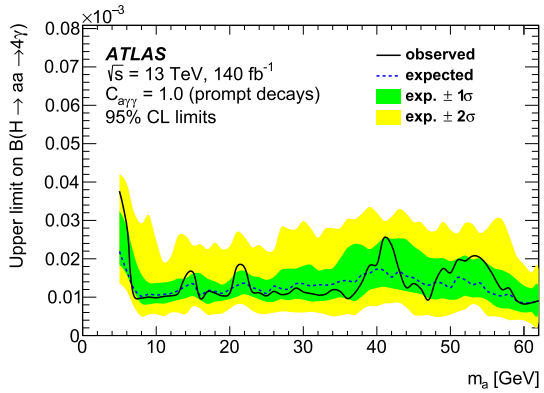

Fig. 8 Upper limits on $\mathcal{B}(H \to aa \to 4\gamma)$ at 95% CL as a function of the signal mass hypothesis and for the assumption of promptly decaying ALPs

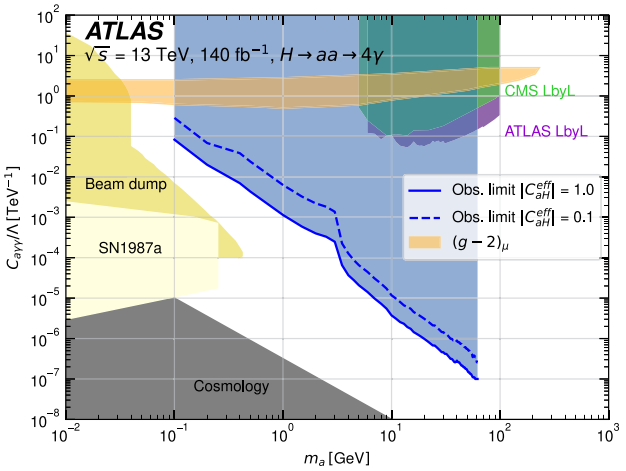

Fig. 9 Limits on the ALP mass and coupling to photons at 95% CL, assuming $\mathcal{B}(a \to \gamma\gamma) = 1$, $\Lambda = 1$ TeV with $|C_{aH}^{\text{eff}}| = 1$ (solid line) and $|C_{aH}^{\text{eff}}| = 0.1$ (dashed line) as predicted in Ref. [19]. The shaded blue area represents the excluded region. The nearly horizontal orange shaded area indicates the region favoured by an ALP explanation for the $(g-2)_\mu$ discrepancy [19]. Also shown are exclusion limits from the respective ATLAS [67] and CMS [68] Light-by-Light (LbyL) scattering analysis, and beam dump experiments, supernova SN1987a and cosmological observations adapted from Ref. [69]

better sensitivity than previous analyses from CMS [28] using 132 fb^{-1} of $\sqrt{s} = 13$ TeV data. These are the first limits on ALPs with masses below 10 GeV from the ATLAS experiment, and are up to 40% more stringent than previous results from CMS [27] using 136 fb^{-1} of $\sqrt{s} = 13$ TeV data. The limits on long-lived ALPs in anomalous Higgs boson decays are the first obtained by any experiment.

The limit on the branching ratio can be converted into a limit on the coupling of axion-like particles to photons, $C_{a\gamma\gamma}$. The branching ratio, which depends on $C_{a\gamma\gamma}$, can be calculated using the method described in Ref. [19]:

$$\mathcal{B}^{\text{theo}} = \Gamma_{Haa} f_{aa}^2(C_{a\gamma\gamma}) \frac{\mathcal{B}(a \to \gamma\gamma)}{\Gamma_H + \Gamma_{Haa}}, \tag{3}$$

where it is assumed that all ALPs decay into photons and hence $\mathcal{B}(a \to \gamma\gamma) = 1$. In the following m_a and m_H refer to the masses of the ALP and Higgs boson, respectively, v is the vacuum expectation value, and the effective coupling of the ALP to the Higgs boson is assumed to be $C_{aH}^{\text{eff}}/\Lambda^2 = 1\,\text{TeV}^{-2}$. Γ_H is the total decay width of the Higgs boson. The Higgs boson to ALP decay width Γ_{Haa} is calculated as

$$\Gamma_{Haa} = \frac{v^2 m_H^3}{32\pi} \frac{|C_{aH}^{\text{eff}}|^2}{\Lambda^4} \left(1 - \frac{2m_a^2}{m_H^2}\right)^2 \sqrt{1 - \frac{4m_a^2}{m_H^2}}. \tag{4}$$

Using the Higgs mass of $m_H = 125$ GeV and assuming $m_a = 10$ GeV and $C_{aH}^{\text{eff}}/\Lambda^2 = 1\,\text{TeV}^{-2}$ yields a branching ratio of the $H \to aa$ process of 30%. The factor $f_{aa}^2(C_{a\gamma\gamma})$ represents the fraction of ALPs detected inside the detector volume. It depends on the ALP decay length, and hence on $C_{a\gamma\gamma}$, since the decay width is given by

$$\Gamma_{a\gamma\gamma} = \frac{4\pi\alpha^2 m_a^3}{\Lambda^2} |C_{a\gamma\gamma}|^2. \tag{5}$$

f_{aa} is determined from the signal simulation and interpolated between the simulated $C_{a\gamma\gamma}$ values. The coupling is adjusted until the expected branching ratio matches the observed limit on the branching ratio, yielding the corresponding limit on $C_{a\gamma\gamma}$.

The resulting limits are shown in the two-dimensional exclusion plot of $C_{a\gamma\gamma}$ vs. m_a presented in Fig. 9. This search significantly reduces the allowed parameter space for ALP-based models that could explain the $(g-2)_\mu$ discrepancy in the $H \to aa \to 4\gamma$ decay mode, as suggested in Ref. [19].

8 Conclusion

This paper reports a search for a light pseudoscalar particle (a) produced in the decay $H \to aa$, where H is the 125 GeV Higgs boson. The a boson, which can have a short or long lifetime, decays into two photons, resulting in a final state with four photons with an invariant mass near 125 GeV. The analysis uses 140 fb^{-1} of pp collision data at a centre-of-mass energy of 13 TeV collected by the ATLAS detector between 2015 and 2018. The search aims to identify a narrow $a \to \gamma\gamma$ resonance with a mass in the range of 100 MeV to 62 GeV, where the resonance decay occurs within a distance of 1970 mm from the collision vertex. Dedicated search strategies for long-lived $a \to \gamma\gamma$ decays are developed for the first time. To enable the search for low resonance masses, neural network classifiers are trained to distinguish between single and collimated photon signatures.

No significant excess over the Standard Model backgrounds is observed in the data. The largest deviation from the expected limit, 1.5σ, is observed in the range of 10 GeV $< m_a <$ 25 GeV. Upper limits at 95% CL are set for $\mathcal{B}(H \to$

$aa \to 4\gamma$), which range from 2×10^{-5} to 3×10^{-2} depending on m_a for the prompt axion-like particle search. For the search for long-lived ALPs with significant displaced decay vertices, upper limits at 95% CL are set, ranging from 2×10^{-5} to 6×10^{-5} for 10 GeV $< m_a <$ 62 GeV and from 10^{-4} to 3×10^{-2} for 0.1 GeV $< m_a <$ 10 GeV. These are the most stringent limits to date.

Acknowledgements We thank CERN for the very successful operation of the LHC and its injectors, as well as the support staff at CERN and at our institutions worldwide without whom ATLAS could not be operated efficiently. The crucial computing support from all WLCG partners is acknowledged gratefully, in particular from CERN, the ATLAS Tier-1 facilities at TRIUMF/SFU (Canada), NDGF (Denmark, Norway, Sweden), CC-IN2P3 (France), KIT/GridKA (Germany), INFN-CNAF (Italy), NL-T1 (Netherlands), PIC (Spain), RAL (UK) and BNL (USA), the Tier-2 facilities worldwide and large non-WLCG resource providers. Major contributors of computing resources are listed in Ref. [70]. We gratefully acknowledge the support of ANPCyT, Argentina; YerPhI, Armenia; ARC, Australia; BMWFW and FWF, Austria; ANAS, Azerbaijan; CNPq and FAPESP, Brazil; NSERC, NRC and CFI, Canada; CERN; ANID, Chile; CAS, MOST and NSFC, China; Minciencias, Colombia; MEYS CR, Czech Republic; DNRF and DNSRC, Denmark; IN2P3-CNRS and CEA-DRF/IRFU, France; SRNSFG, Georgia; BMBF, HGF and MPG, Germany; GSRI, Greece; RGC and Hong Kong SAR, China; ISF and Benoziyo Center, Israel; INFN, Italy; MEXT and JSPS, Japan; CNRST, Morocco; NWO, Netherlands; RCN, Norway; MEiN, Poland; FCT, Portugal; MNE/IFA, Romania; MESTD, Serbia; MSSR, Slovakia; ARRS and MIZŠ, Slovenia; DSI/NRF, South Africa; MICINN, Spain; SRC and Wallenberg Foundation, Sweden; SERI, SNSF and Cantons of Bern and Geneva, Switzerland; MOST, Taipei; TENMAK, Türkiye; STFC, United Kingdom; DOE and NSF, United States of America. Individual groups and members have received support from BCKDF, CANARIE, CRC and DRAC, Canada; CERN-CZ, PRIMUS 21/SCI/017 and UNCE SCI/013, Czech Republic; COST, ERC, ERDF, Horizon 2020, ICSC-NextGenerationEU and Marie Skłodowska-Curie Actions, European Union; Investissements d'Avenir Labex, Investissements d'Avenir Idex and ANR, France; DFG and AvH Foundation, Germany; Herakleitos, Thales and Aristeia programmes co-financed by EU-ESF and the Greek NSRF, Greece; BSF-NSF and MINERVA, Israel; Norwegian Financial Mechanism 2014-2021, Norway; NCN and NAWA, Poland; La Caixa Banking Foundation, CERCA Programme Generalitat de Catalunya and PROMETEO and GenT Programmes Generalitat Valenciana, Spain; Göran Gustafssons Stiftelse, Sweden; The Royal Society and Leverhulme Trust, United Kingdom. In addition, individual members wish to acknowledge support from Chile: Agencia Nacional de Investigación y Desarrollo (FONDECYT 1190886, FONDECYT 1210400, FONDECYT 1230987); China: National Natural Science Foundation of China (NSFC-12175119, NSFC 12275265, NSFC-12075060); European Union: European Research Council (ERC - 948254), Horizon 2020 Framework Programme (MUCCA - CHIST-ERA-19-XAI-00), Italian Center for High Performance Computing, Big Data and Quantum Computing (ICSC, NextGenerationEU), Marie Sklodowska-Curie Actions (EU H2020 MSC IF GRANT NO 101033496); France: Agence Nationale de la Recherche (ANR-20-CE31-0013, ANR-21-CE31-0013, ANR-21-CE31-0022), Investissements d'Avenir Idex (ANR-11-LABX-0012), Investissements d'Avenir Labex (ANR-11-LABX-0012); Germany: Baden-Württemberg Stiftung (BW Stiftung-Postdoc Eliteprogramme), Deutsche Forschungsgemeinschaft (DFG-CR 312/5-1); Italy: Istituto Nazionale di Fisica Nucleare (FELLINI G.A. n. 754496, ICSC, NextGenerationEU); Japan: Japan Society for the Promotion of Science (JSPS KAKENHI JP21H05085, JSPS KAKENHI JP22H01227, JSPS KAKENHI JP22H04944); Netherlands: Netherlands Organisation for Scientific Research (NWO Veni 2020 - VI.Veni.202.179); Norway: Research Council of Norway (RCN-314472); Poland: Polish National Agency for Academic Exchange (PPN/PPO/2020/1/00002/U/00001), Polish National Science Centre (NCN 2021/42/E/ST2/00350, NCN UMO-2019/34/E/ST2/00393, UMO-2020/37/B/ST2/01043, UMO-2021/40/C/ST2/00187); Slovenia: Slovenian Research Agency (ARIS grant J1-3010); Spain: BBVA Foundation (LEO22-1-603), Generalitat Valenciana (Artemisa, FEDER, IDIFEDER/2018/048), La Caixa Banking Foundation (LCF/BQ/PI20/11760025), Ministry of Science and Innovation (MCIN and NextGenEU - PCI2022-135018-2, MICIN and FEDER -PID2021-125273NB, RYC2019-028510-I, RYC2020-030254-I), PROMETEO and GenT Programmes Generalitat Valenciana (CIDEGENT/2019/023, CIDEGENT/2019/027); Sweden: Swedish Research Council (VR 2018-00482, VR 2022-03845, VR 2022-04683, VR grant 2021-03651), Knut and Alice Wallenberg Foundation (KAW 2017.0100, KAW 2018.0157, KAW 2018.0458, KAW 2019.0447); Switzerland: Swiss National Science Foundation (SNSF-PCEFP2_194658); United Kingdom: Leverhulme Trust (Leverhulme Trust RPG-2020-004); United States of America: Neubauer Family Foundation.

Data Availability Statement This manuscript has no associated data. [Authors' comment: Data sharing not applicable to this article as no datasets were generated or analysed during the current study.]

Code Availability Statement This manuscript has no associated code/software. [Authors' comment: Code/Software sharing not applicable to this article as no code/software was generated or analysed during the current study.]

Open Access This article is licensed under a Creative Commons Attribution 4.0 International License, which permits use, sharing, adaptation, distribution and reproduction in any medium or format, as long as you give appropriate credit to the original author(s) and the source, provide a link to the Creative Commons licence, and indicate if changes were made. The images or other third party material in this article are included in the article's Creative Commons licence, unless indicated otherwise in a credit line to the material. If material is not included in the article's Creative Commons licence and your intended use is not permitted by statutory regulation or exceeds the permitted use, you will need to obtain permission directly from the copyright holder. To view a copy of this licence, visit http://creativecommons.org/licenses/by/4.0/.
Funded by SCOAP[3].

References

1. ATLAS Collaboration, Observation of a new particle in the search for the Standard Model Higgs boson with the ATLAS detector at the LHC. Phys. Lett. B **716**, 1 (2012). https://doi.org/10.1016/j.physletb.2012.08.020. arXiv:1207.7214 [hep-ex]
2. CMS Collaboration, Observation of a new boson at a mass of 125 GeV with the CMS experiment at the LHC. Phys. Lett. B **716**, 30 (2012). https://doi.org/10.1016/j.physletb.2012.08.021. arXiv:1207.7235 [hep-ex]
3. B.A. Dobrescu, K.T. Matchev, Light axion within the next-to-minimal supersymmetric standard model. JHEP **09**, 031 (2000). https://doi.org/10.1088/1126-6708/2000/09/031. arXiv:hep-ph/0008192
4. U. Ellwanger, J.F. Gunion, C. Hugonie, S. Moretti, Towards a no-lose theorem for NMSSM Higgs discovery at the LHC. (2003). arXiv:hep-ph/0305109
5. S. Profumo, M.J. Ramsey-Musolf, G. Shaughnessy, Singlet Higgs phenomenology and the electroweak phase transition. JHEP

08, 010 (2007). https://doi.org/10.1088/1126-6708/2007/08/010. arXiv:0705.2425 [hep-ph]
6. N. Blinov, J. Kozaczuk, D.E. Morrissey, C. Tamarit, Electroweak baryogenesis from exotic electroweak symmetry breaking. Phys. Rev. D **92**, 035012 (2015). https://doi.org/10.1103/PhysRevD.92.035012. arXiv:1504.05195 [hep-ph]
7. N. Craig, A. Katz, M. Strassler, R. Sundrum, Naturalness in the dark at the LHC. JHEP **07**, 105 (2015). https://doi.org/10.1007/JHEP07(2015)105. arXiv:1501.05310 [hep-ph]
8. D. Curtin, C.B. Verhaaren, Discovering uncolored naturalness in exotic Higgs decays. JHEP **12**, 072 (2015). https://doi.org/10.1007/JHEP12(2015)072. arXiv:1506.06141 [hep-ph]
9. V. Silveira, A. Zee, Scalar phantoms. Phys. Lett. B **161**, 136 (1985). https://doi.org/10.1016/0370-2693(85)90624-0
10. M. Pospelov, A. Ritz, M. Voloshin, Secluded WIMP dark matter. Phys. Lett. B **662**, 53 (2008). https://doi.org/10.1016/j.physletb.2008.02.052. arXiv:0711.4866 [hep-ph]
11. P. Draper, T. Liu, C.E.M. Wagner, L.-T. Wang, H. Zhang, Dark light-Higgs bosons. Phys. Rev. Lett. **106**, 121805 (2011). https://doi.org/10.1103/PhysRevLett.106.121805. arXiv:1009.3963 [hep-ph]
12. S. Ipek, D. McKeen, A.E. Nelson, Renormalizable model for the Galactic Center gamma-ray excess from dark matter annihilation. Phys. Rev. D **90**, 055021 (2014). https://doi.org/10.1103/PhysRevD.90.055021. arXiv:1404.3716 [hep-ph]
13. A. Martin, J. Shelton, J. Unwin, Fitting the galactic center gamma-ray excess with cascade annihilations. Phys. Rev. D **90**, 103513 (2014). https://doi.org/10.1103/PhysRevD.90.103513. arXiv:1405.0272 [hep-ph]
14. C. Boehm, M.J. Dolan, C. McCabe, M. Spannowsky, C.J. Wallace, Extended gamma-ray emission from Coy Dark Matter. JCAP **05**, 009 (2014). https://doi.org/10.1088/1475-7516/2014/05/009. arXiv:1401.6458 [hep-ph]
15. D. Curtin et al., Exotic decays of the 125 GeV Higgs boson. Phys. Rev. D **90**, 075004 (2014). https://doi.org/10.1103/PhysRevD.90.075004. arXiv:1312.4992 [hep-ph]
16. ATLAS Collaboration, Combination of searches for invisible decays of the Higgs boson using 139 fb^{-1} of proton-proton collision data at $\sqrt{s} = 13$ TeV collected with the ATLAS experiment. Phys. Lett. B **842**, 137963 (2023). https://doi.org/10.1016/j.physletb.2023.137963. arXiv:2301.10731 [hep-ex]
17. ATLAS Collaboration, A detailed map of Higgs boson interactions by the ATLAS experiment ten years after the discovery, Nature **607**, 52 (2022). https://doi.org/10.1038/s41586-022-04893-w. arXiv:2207.00092 [hep-ex] [Erratum: Nature 612 (2022) E24 https://doi.org/10.1038/s41586-022-05581-5]
18. CMS Collaboration, A portrait of the Higgs boson by the CMS experiment ten years after the discovery. Nature **607**, 60 (2022). https://doi.org/10.1038/s41586-022-04892-x. arXiv:2207.00043 [hep-ex]
19. M. Bauer, M. Neubert, A. Thamm, Collider probes of axion-like particles. JHEP **12**, 044 (2017). https://doi.org/10.1007/JHEP12(2017)044. arXiv:1708.00443 [hep-ph]
20. Muon g-2 Collaboration, Measurement of the positive muon anomalous magnetic moment to 0.46 ppm. Phys. Rev. Lett. **126**, 141801 (2021). https://doi.org/10.1103/PhysRevLett.126.141801. arXiv:2104.03281 [hep-ex]
21. Muon g-2 Collaboration, Final report of the E821 muon anomalous magnetic moment measurement at BNL. Phys. Rev. D **73**, 072003 (2006). https://doi.org/10.1103/PhysRevD.73.072003. arXiv:hep-ex/0602035
22. D.P. Aguillard et al., Measurement of the positive muon anomalous magnetic moment to 0.20 ppm. (2023). arXiv:2308.06230 [hep-ex]
23. T. Aoyama et al., The anomalous magnetic moment of the muon in the Standard Model. Phys. Rep. **887**, 1 (2020). https://doi.org/10.1016/j.physrep.2020.07.006. arXiv:2006.04822 [hep-ph]
24. RBC and UKQCD Collaborations, Calculation of the hadronic vacuum polarization contribution to the muon anomalous magnetic moment. Phys. Rev. Lett. **121**, 022003 (2018). https://doi.org/10.1103/PhysRevLett.121.022003. arXiv:1801.07224 [hep-lat]
25. L. Evans, P. Bryant, L.H.C. Machine, JINST **3**, S08001 (2008). https://doi.org/10.1088/1748-0221/3/08/S08001
26. ATLAS Collaboration, Search for new phenomena in events with at least three photons collected in pp collisions at $\sqrt{s} = 8$ TeV with the ATLAS detector. Eur. Phys. J. C **76**, 210 (2016). https://doi.org/10.1140/epjc/s10052-016-4034-8. arXiv:1509.05051 [hep-ex]
27. CMS Collaboration, Search for exotic Higgs boson decays $H \to \mathcal{A}\mathcal{A} \to 4\gamma$ with events containing two merged diphotons in proton-proton collisions at $\sqrt{s}$ = 13 TeV. Phys. Rev. Lett. **131**, 101801 (2023). https://doi.org/10.1103/PhysRevLett.131.101801. arXiv:2209.06197 [hep-ex]
28. CMS Collaboration, Search for the exotic decay of the Higgs boson into two light pseudoscalars with four photons in the final state in proton-proton collisions at $\sqrt{s}$ = 13 TeV. JHEP **07**, 148 (2023). https://doi.org/10.1007/JHEP07(2023)148. arXiv:2208.01469 [hep-ex]
29. ATLAS Collaboration, The ATLAS Experiment at the CERN Large Hadron Collider. JINST **3**, S08003 (2008). https://doi.org/10.1088/1748-0221/3/08/S08003
30. ATLAS Collaboration, ATLAS Insertable B-Layer: Technical Design Report, ATLAS-TDR-19; CERN-LHCC-2010-013. (2010). https://cds.cern.ch/record/1291633, Addendum: ATLAS-TDR-19-ADD-1; CERN-LHCC-2012-009. (2012). https://cds.cern.ch/record/1451888
31. B. Abbott et al., Production and integration of the ATLAS Insertable B-Layer. JINST **13**, T05008 (2018). https://doi.org/10.1088/1748-0221/13/05/T05008. arXiv:1803.00844 [physics.ins-det]
32. ATLAS Collaboration, Performance of the ATLAS trigger system in 2015. Eur. Phys. J. C **77**(2017), 317 (2017). https://doi.org/10.1140/epjc/s10052-017-4852-3. arXiv:1611.09661 [hep-ex]
33. ATLAS Collaboration, The ATLAS Collaboration Software and Firmware, ATL-SOFT-PUB-2021-001. (2021). https://cds.cern.ch/record/2767187
34. ATLAS Collaboration, ATLAS data quality operations and performance for 2015–2018 data-taking. JINST **15**, P04003 (2020). https://doi.org/10.1088/1748-0221/15/04/P04003. arXiv:1911.04632 [physics.ins-det]
35. ATLAS Collaboration, Luminosity determination in pp collisions at $\sqrt{s} = 13$ TeV using the ATLAS detector at the LHC. Eur. Phys. J. C **83**, 982 (2023). https://doi.org/10.1140/epjc/s10052-023-11747-w. arXiv:2212.09379 [hep-ex]
36. M. Aaboud et al., Measurement of the production cross section of three isolated photons in pp collisions at $\sqrt{s}$ = 8 TeV using the ATLAS detector. Phys. Lett. B **781**, 55 (2018). https://doi.org/10.1016/j.physletb.2018.03.057. arXiv:1712.07291 [hep-ex]
37. T. Gleisberg et al., Event generation with SHERPA 1.1. JHEP **02**, 007 (2009). https://doi.org/10.1088/1126-6708/2009/02/007. arXiv:0811.4622 [hep-ph]
38. E. Bothmann et al., Event generation with Sherpa 22. SciPost Phys. **7**, 034 (2019). https://doi.org/10.21468/SciPostPhys.7.3.034. arXiv:1905.09127 [hep-ph]
39. S. Höche, F. Krauss, S. Schumann, F. Siegert, QCD matrix elements and truncated showers. JHEP **05**, 053 (2009). https://doi.org/10.1088/1126-6708/2009/05/053. arXiv:0903.1219 [hep-ph]
40. ATLAS Collaboration, Measurement of the Z/γ^* boson transverse momentum distribution in pp collisions at $\sqrt{s} = 7\,TeV$ with the ATLAS detector. JHEP **09**, 145 (2014). https://doi.org/10.1007/JHEP09(2014)145. arXiv:1406.3660 [hep-ex]
41. NNPDF Collaboration, R.D. Ball et al., Parton distributions for the LHC run II. JHEP **04**, 040 (2015). https://doi.org/10.1007/JHEP04(2015)040. arXiv:1410.8849 [hep-ph]

42. P. Nason, A new method for combining NLO QCD with shower Monte Carlo algorithms. JHEP **11**, 040 (2004). https://doi.org/10.1088/1126-6708/2004/11/040. arXiv:hep-ph/0409146
43. S. Frixione, P. Nason, C. Oleari, Matching NLO QCD computations with parton shower simulations: the POWHEG method. JHEP **11**, 070 (2007). https://doi.org/10.1088/1126-6708/2007/11/070. arXiv:0709.2092 [hep-ph]
44. S. Alioli, P. Nason, C. Oleari, E. Re, A general framework for implementing NLO calculations in shower Monte Carlo programs: the POWHEG BOX. JHEP **06**, 043 (2010). https://doi.org/10.1007/JHEP06(2010)043. arXiv:1002.2581 [hep-ph]
45. T. Sjöstrand et al., An introduction to PYTHIA 8.2. Comput. Phys. Commun. **191**, 159 (2015). https://doi.org/10.1016/j.cpc.2015.01.024. arXiv:1410.3012 [hep-ph]
46. D. de Florian et al., Handbook of LHC Higgs Cross Sections: 4. Deciphering the nature of the Higgs sector. (2016) https://doi.org/10.23731/CYRM-2017-002. arXiv:1610.07922 [hep-ph]
47. C. Anastasiou et al., High precision determination of the gluon fusion Higgs boson cross-section at the LHC. JHEP **05**, 058 (2016). https://doi.org/10.1007/JHEP05(2016)058. arXiv:1602.00695 [hep-ph]
48. S. Actis, G. Passarino, C. Sturm, S. Uccirati, NLO electroweak corrections to Higgs boson production at hadron colliders. Phys. Lett. B **670**, 12 (2008). https://doi.org/10.1016/j.physletb.2008.10.018. arXiv:0809.1301 [hep-ph]
49. C. Anastasiou, R. Boughezal, F. Petriello, Mixed QCD-electroweak corrections to Higgs boson production in gluon fusion. JHEP **04**, 003 (2009). https://doi.org/10.1088/1126-6708/2009/04/003. arXiv:0811.3458 [hep-ph]
50. B. Grzadkowski, H.E. Haber, O.M. Ogreid, P. Osland, Heavy Higgs boson decays in the alignment limit of the 2HDM. JHEP **12**, 056 (2018). https://doi.org/10.1007/JHEP12(2018)056. arXiv:1808.01472 [hep-ph]
51. D. Stump et al., Inclusive jet production, parton distributions, and the search for new physics. JHEP **10**, 046 (2003). https://doi.org/10.1088/1126-6708/2003/10/046. arXiv:hep-ph/0303013
52. NNPDF Collaboration, R. D. Ball et al., Parton distributions with LHC data. Nucl. Phys. B **867**, 244 (2013). https://doi.org/10.1016/j.nuclphysb.2012.10.003. arXiv:1207.1303 [hep-ph]
53. ATLAS Collaboration, The Pythia 8 A3 tune description of ATLAS minimum bias and inelastic measurements incorporating the Donnachie–Landshoff diffractive model, ATL-PHYS-PUB-2016-017. (2016). https://cds.cern.ch/record/2206965
54. ATLAS Collaboration, The ATLAS simulation infrastructure. Eur. Phys. J. C **70**, 823 (2010). https://doi.org/10.1140/epjc/s10052-010-1429-9. arXiv:1005.4568 [physics.ins-det]
55. S. Agostinelli et al., Geant4—a simulation toolkit. Nucl. Instrum. Methods A **506**, 250 (2003). https://doi.org/10.1016/S0168-9002(03)01368-8
56. ATLAS Collaboration, Electron and photon reconstruction and performance in ATLAS using a dynamical, topological cell clustering-based approach, ATL-PHYS-PUB-2017-022. (2017). https://cds.cern.ch/record/2298955
57. ATLAS Collaboration, Electron and photon efficiencies in LHC Run 2 with the ATLAS experiment. (2023). arXiv:2308.13362 [hep-ex]
58. ATLAS Collaboration, Electron and photon performance measurements with the ATLAS detector using the 2015–2017 LHC proton–proton collision data. JINST **14**, P12006 (2019). https://doi.org/10.1088/1748-0221/14/12/P12006. arXiv:1908.00005 [hep-ex]
59. ATLAS Collaboration, Electron and photon energy calibration with the ATLAS detector using LHC Run 2 data. (2023). arXiv:2309.05471 [hep-ex]
60. ATLAS Collaboration, Performance of electron and photon triggers in ATLAS during LHC Run 2. Eur. Phys. J. C **80**, 47 (2020). https://doi.org/10.1140/epjc/s10052-019-7500-2. arXiv:1909.00761 [hep-ex]
61. G. Avoni et al., The new LUCID-2 detector for luminosity measurement and monitoring in ATLAS. JINST **13**, P07017 (2018). https://doi.org/10.1088/1748-0221/13/07/P07017
62. ATLAS Collaboration, Recommendations for the Modeling of Smooth Backgrounds, ATL-PHYS-PUB-2020-028. (2020). https://cds.cern.ch/record/2743717
63. J. Baglio et al., $gg \to HH$: combined uncertainties. Phys. Rev. D **103**, 056002 (2021). https://doi.org/10.1103/PhysRevD.103.056002. arXiv:2008.11626 [hep-ph]
64. L. Heinrich, M. Feickert, G. Stark, K. Cranmer, pyhf: pure-Python implementation of HistFactory statistical models. J. Open Source Softw. **6**, 2823 (2021). https://doi.org/10.21105/joss.02823
65. L. Heinrich, M. Feickert, G. Stark, pyhf: v0.7.1, version 0.7.1. https://github.com/scikit-hep/pyhf/releases/tag/v0.7.1. https://doi.org/10.5281/zenodo.1169739
66. A.L. Read, Presentation of search results: the CL_S technique. J. Phys. G **28**, 2693 (2002). https://doi.org/10.1088/0954-3899/28/10/313
67. ATLAS Collaboration, Measurement of light-by-light scattering and search for axion-like particles with 2.2 nb^{-1} of $Pb + Pb$ data with the ATLAS detector. JHEP **03**, 243 (2021). https://doi.org/10.1007/JHEP03(2021)243. arXiv:2008.05355 [hep-ex], Erratum: JHEP 11 (2021) 050 https://doi.org/10.1007/JHEP11(2021)050
68. CMS Collaboration, Evidence for light-by-light scattering and searches for axion-like particles in ultraperipheral PbPb collisions at $\sqrt{s_{NN}} = 5.02$, TeV. Phys. Lett. B **797**, 134826 (2019). https://doi.org/10.1016/j.physletb.2019.134826. arXiv:1810.04602 [hep-ex]
69. J. Jaeckel, M. Spannowsky, Probing MeV to 90 GeV axion-like particles with LEP and LHC. Phys. Lett. B **753**, 482 (2016). https://doi.org/10.1016/j.physletb.2015.12.037. arXiv:1509.00476 [hep-ph]
70. ATLAS Collaboration, ATLAS Computing Acknowledgements, ATL-SOFT-PUB-2023-001. (2023). https://cds.cern.ch/record/2869272

ATLAS Collaboration[*]

G. Aad[102], B. Abbott[120], K. Abeling[55], N. J. Abicht[49], S. H. Abidi[29], A. Aboulhorma[35e], H. Abramowicz[151], H. Abreu[150], Y. Abulaiti[117], B. S. Acharya[69a,69b,m], C. Adam Bourdarios[4], L. Adamczyk[86a], S. V. Addepalli[26], M. J. Addison[101], J. Adelman[115], A. Adiguzel[21c], T. Adye[134], A. A. Affolder[136], Y. Afik[36], M. N. Agaras[13], J. Agarwala[73a,73b], A. Aggarwal[100], C. Agheorghiesei[27c], A. Ahmad[36], F. Ahmadov[38,y], W. S. Ahmed[104], S. Ahuja[95], X. Ai[62a], G. Aielli[76a,76b], A. Aikot[163], M. Ait Tamlihat[35e], B. Aitbenchikh[35a], I. Aizenberg[169], M. Akbiyik[100], T. P. A. Åkesson[98], A. V. Akimov[37], D. Akiyama[168], N. N. Akolkar[24], K. Al Khoury[41], G. L. Alberghi[23b], J. Albert[165], P. Albicocco[53], G. L. Albouy[60], S. Alderweireldt[52], M. Aleksa[36], I. N. Aleksandrov[38], C. Alexa[27b], T. Alexopoulos[10], F. Alfonsi[23b], M. Algren[56], M. Alhroob[120], B. Ali[132], H. M. J. Ali[91], S. Ali[148], S. W. Alibocus[92], M. Aliev[145], G. Alimonti[71a], W. Alkakhi[55], C. Allaire[66], B. M. M. Allbrooke[146], J. F. Allen[52], C. A. Allendes Flores[137f], P. P. Allport[20], A. Aloisio[72a,72b], F. Alonso[90], C. Alpigiani[138], M. Alvarez Estevez[99], A. Alvarez Fernandez[100], M. Alves Cardoso[56], M. G. Alviggi[72a,72b], M. Aly[101], Y. Amaral Coutinho[83b], A. Ambler[104], C. Amelung[36], M. Amerl[101], C. G. Ames[109], D. Amidei[106], S. P. Amor Dos Santos[130a], K. R. Amos[163], V. Ananiev[125], C. Anastopoulos[139], T. Andeen[11], J. K. Anders[36], S. Y. Andrean[47a,47b], A. Andreazza[71a,71b], S. Angelidakis[9], A. Angerami[41,ab], A. V. Anisenkov[37], A. Annovi[74a], C. Antel[56], M. T. Anthony[139], E. Antipov[145], M. Antonelli[53], F. Anulli[75a], M. Aoki[84], T. Aoki[153], J. A. Aparisi Pozo[163], M. A. Aparo[146], L. Aperio Bella[48], C. Appelt[18], A. Apyan[26], N. Aranzabal[36], S. J. Arbiol Val[87], C. Arcangeletti[53], A. T. H. Arce[51], E. Arena[92], J-F. Arguin[108], S. Argyropoulos[54], J.-H. Arling[48], O. Arnaez[4], H. Arnold[114], G. Artoni[75a,75b], H. Asada[111], K. Asai[118], S. Asai[153], N. A. Asbah[61], K. Assamagan[29], R. Astalos[28a], S. Atashi[160], R. J. Atkin[33a], M. Atkinson[162], H. Atmani[35f], P. A. Atmasiddha[106], K. Augsten[132], S. Auricchio[72a,72b], A. D. Auriol[20], V. A. Austrup[101], G. Avolio[36], K. Axiotis[56], G. Azuelos[108,af], D. Babal[28b], H. Bachacou[135], K. Bachas[152,p], A. Bachiu[34], F. Backman[47a,47b], A. Badea[61], T. M. Baer[106], P. Bagnaia[75a,75b], M. Bahmani[18], A. J. Bailey[163], V. R. Bailey[162], J. T. Baines[134], L. Baines[94], O. K. Baker[172], E. Bakos[15], D. Bakshi Gupta[8], V. Balakrishnan[120], R. Balasubramanian[114], E. M. Baldin[37], P. Balek[86a], E. Ballabene[23a,23b], F. Balli[135], L. M. Baltes[63a], W. K. Balunas[32], J. Balz[100], E. Banas[87], M. Bandieramonte[129], A. Bandyopadhyay[24], S. Bansal[24], L. Barak[151], M. Barakat[48], E. L. Barberio[105], D. Barberis[57a,57b], M. Barbero[102], M. Z. Barel[114], K. N. Barends[33a], T. Barillari[110], M-S. Barisits[36], T. Barklow[143], P. Baron[122], D. A. Baron Moreno[101], A. Baroncelli[62a], G. Barone[29], A. J. Barr[126], J. D. Barr[96], L. Barranco Navarro[47a,47b], F. Barreiro[99], J. Barreiro Guimarães da Costa[14a], U. Barron[151], M. G. Barros Teixeira[130a], S. Barsov[37], F. Bartels[63a], R. Bartoldus[143], A. E. Barton[91], P. Bartos[28a], A. Basan[100], M. Baselga[49], A. Bassalat[66,b], M. J. Basso[156a], C. R. Basson[101], R. L. Bates[59], S. Batlamous[35e], J. R. Batley[32], B. Batool[141], M. Battaglia[136], D. Battulga[18], M. Bauce[75a,75b], M. Bauer[36], P. Bauer[24], L. T. Bazzano Hurrell[30], J. B. Beacham[51], T. Beau[127], J. Y. Beaucamp[90], P. H. Beauchemin[158], F. Becherer[54], P. Bechtle[24], H. P. Beck[19,o], K. Becker[167], A. J. Beddall[82], V. A. Bednyakov[38], C. P. Bee[145], L. J. Beemster[15], T. A. Beermann[36], M. Begalli[83d], M. Begel[29], A. Behera[145], J. K. Behr[48], J. F. Beirer[55], F. Beisiegel[24], M. Belfkir[159], G. Bella[151], L. Bellagamba[23b], A. Bellerive[34], P. Bellos[20], K. Beloborodov[37], D. Benchekroun[35a], F. Bendebba[35a], Y. Benhammou[151], M. Benoit[29], J. R. Bensinger[26], S. Bentvelsen[114], L. Beresford[48], M. Beretta[53], E. Bergeaas Kuutmann[161], N. Berger[4], B. Bergmann[132], J. Beringer[17a], G. Bernardi[5], C. Bernius[143], F. U. Bernlochner[24], F. Bernon[36,102], A. Berrocal Guardia[13], T. Berry[95], P. Berta[133], A. Berthold[50], I. A. Bertram[91], S. Bethke[110], A. Betti[75a,75b], A. J. Bevan[94], N. K. Bhalla[54], M. Bhamjee[33c], S. Bhatta[145], D. S. Bhattacharya[166], P. Bhattarai[143], V. S. Bhopatkar[121], R. Bi[29,ai], R. M. Bianchi[129], G. Bianco[23b,23a], O. Biebel[109], R. Bielski[123], M. Biglietti[77a], M. Bindi[55], A. Bingul[21b], C. Bini[75a,75b], A. Biondini[92], C. J. Birch-sykes[101], G. A. Bird[20,134], M. Birman[169], M. Biros[133], S. Biryukov[146], T. Bisanz[49], E. Bisceglie[43a,43b], J. P. Biswal[134], D. Biswas[141], A. Bitadze[101], K. Bjørke[125], I. Bloch[48], C. Blocker[26], A. Blue[59], U. Blumenschein[94], J. Blumenthal[100], G. J. Bobbink[114], V. S. Bobrovnikov[37], M. Boehler[54], B. Boehm[166], D. Bogavac[36], A. G. Bogdanchikov[37], C. Bohm[47a], V. Boisvert[95], P. Bokan[48], T. Bold[86a], M. Bomben[5], M. Bona[94], M. Boonekamp[135], C. D. Booth[95], A. G. Borbély[59], I. S. Bordulev[37], H. M. Borecka-Bielska[108], G. Borissov[91], D. Bortoletto[126], D. Boscherini[23b], M. Bosman[13], J. D. Bossio Sola[36], K. Bouaouda[35a], N. Bouchhar[163], J. Boudreau[129], E. V. Bouhova-Thacker[91], D. Boumediene[40], R. Bouquet[165], A. Boveia[119], J. Boyd[36], D. Boye[29], I. R. Boyko[38], J. Bracinik[20], N. Brahimi[62d], G. Brandt[171], O. Brandt[32], F. Braren[48], B. Brau[103], J. E. Brau[123], R. Brener[169], L. Brenner[114], R. Brenner[161], S. Bressler[169], D. Britton[59], D. Britzger[110], I. Brock[24], G. Brooijmans[41], W. K. Brooks[137f], E. Brost[29], L. M. Brown[165], L. E. Bruce[61], T. L. Bruckler[126], P. A. Bruckman de Renstrom[87], B. Brüers[48], A. Bruni[23b], G. Bruni[23b], M.

Bruschi[23b], N. Bruscino[75a,75b], T. Buanes[16], Q. Buat[138], D. Buchin[110], A. G. Buckley[59], O. Bulekov[37], B. A. Bullard[143], S. Burdin[92], C. D. Burgard[49], A. M. Burger[40], B. Burghgrave[8], O. Burlayenko[54], J. T. P. Burr[32], C. D. Burton[11], J. C. Burzynski[142], E. L. Busch[41], V. Büscher[100], P. J. Bussey[59], J. M. Butler[25], C. M. Buttar[59], J. M. Butterworth[96], W. Buttinger[134], C. J. Buxo Vazquez[107], A. R. Buzykaev[37], S. Cabrera Urbán[163], L. Cadamuro[66], D. Caforio[58], H. Cai[129], Y. Cai[14a,14e], Y. Cai[14c], V. M. M. Cairo[36], O. Cakir[3a], N. Calace[36], P. Calafiura[17a], G. Calderini[127], P. Calfayan[68], G. Callea[59], L. P. Caloba[83b], D. Calvet[40], S. Calvet[40], T. P. Calvet[102], M. Calvetti[74a,74b], R. Camacho Toro[127], S. Camarda[36], D. Camarero Munoz[26], P. Camarri[76a,76b], M. T. Camerlingo[72a,72b], D. Cameron[36], C. Camincher[165], M. Campanelli[96], A. Camplani[42], V. Canale[72a,72b], A. Canesse[104], J. Cantero[163], Y. Cao[162], F. Capocasa[26], M. Capua[43a,43b], A. Carbone[71a,71b], R. Cardarelli[76a], J. C. J. Cardenas[8], F. Cardillo[163], G. Carducci[43a,43b], T. Carli[36], G. Carlino[72a], J. I. Carlotto[13], B. T. Carlson[129,q], E. M. Carlson[156a,165], L. Carminati[71a,71b], A. Carnelli[135], M. Carnesale[75a,75b], S. Caron[113], E. Carquin[137f], S. Carrá[71a], G. Carratta[23a,23b], F. Carrio Argos[33g], J. W. S. Carter[155], T. M. Carter[52], M. P. Casado[13,i], M. Caspar[48], F. L. Castillo[4], L. Castillo Garcia[13], V. Castillo Gimenez[163], N. F. Castro[130a,130e], A. Catinaccio[36], J. R. Catmore[125], V. Cavaliere[29], N. Cavalli[23a,23b], V. Cavasinni[74a,74b], Y. C. Cekmecelioglu[48], E. Celebi[21a], F. Celli[126], M. S. Centonze[70a,70b], V. Cepaitis[56], K. Cerny[122], A. S. Cerqueira[83a], A. Cerri[146], L. Cerrito[76a,76b], F. Cerutti[17a], B. Cervato[141], A. Cervelli[23b], G. Cesarini[53], S. A. Cetin[82], Z. Chadi[35a], D. Chakraborty[115], J. Chan[170], W. Y. Chan[153], J. D. Chapman[32], E. Chapon[135], B. Chargeishvili[149b], D. G. Charlton[20], T. P. Charman[94], M. Chatterjee[19], C. Chauhan[133], S. Chekanov[6], S. V. Chekulaev[156a], G. A. Chelkov[38,a], A. Chen[106], B. Chen[151], B. Chen[165], H. Chen[14c], H. Chen[29], J. Chen[62c], J. Chen[142], M. Chen[126], S. Chen[153], S. J. Chen[14c], X. Chen[62c,135], X. Chen[14b,ae], Y. Chen[62a], C. L. Cheng[170], H. C. Cheng[64a], S. Cheong[143], A. Cheplakov[38], E. Cheremushkina[48], E. Cherepanova[114], R. Cherkaoui El Moursli[35e], E. Cheu[7], K. Cheung[65], L. Chevalier[135], V. Chiarella[53], G. Chiarelli[74a], N. Chiedde[102], G. Chiodini[70a], A. S. Chisholm[20], A. Chitan[27b], M. Chitishvili[163], M. V. Chizhov[38], K. Choi[11], A. R. Chomont[75a,75b], Y. Chou[103], E. Y. S. Chow[113], T. Chowdhury[33g], K. L. Chu[169], M. C. Chu[64a], X. Chu[14a,14e], J. Chudoba[131], J. J. Chwastowski[87], D. Cieri[110], K. M. Ciesla[86a], V. Cindro[93], A. Ciocio[17a], F. Cirotto[72a,72b], Z. H. Citron[169,k], M. Citterio[71a], D. A. Ciubotaru[27b], B. M. Ciungu[155], A. Clark[56], P. J. Clark[52], C. Clarry[155], J. M. Clavijo Columbie[48], S. E. Clawson[48], C. Clement[47a,47b], J. Clercx[48], Y. Coadou[102], M. Cobal[69a,69c], A. Coccaro[57b], R. F. Coelho Barrue[130a], R. Coelho Lopes De Sa[103], S. Coelli[71a], H. Cohen[151], A. E. C. Coimbra[71a,71b], B. Cole[41], J. Collot[60], P. Conde Muiño[130a,130g], M. P. Connell[33c], S. H. Connell[33c], I. A. Connelly[59], E. I. Conroy[126], F. Conventi[72a,ag], H. G. Cooke[20], A. M. Cooper-Sarkar[126], A. Cordeiro Oudot Choi[127], L. D. Corpe[40], M. Corradi[75a,75b], F. Corriveau[104,w], A. Cortes-Gonzalez[18], M. J. Costa[163], F. Costanza[4], D. Costanzo[139], B. M. Cote[119], G. Cowan[95], K. Cranmer[170], D. Cremonini[23a,23b], S. Crépé-Renaudin[60], F. Crescioli[127], M. Cristinziani[141], M. Cristoforetti[78a,78b], V. Croft[114], J. E. Crosby[121], G. Crosetti[43a,43b], A. Cueto[99], T. Cuhadar Donszelmann[160], H. Cui[14a,14e], Z. Cui[7], W. R. Cunningham[59], F. Curcio[43a,43b], P. Czodrowski[36], M. M. Czurylo[63b], M. J. Da Cunha Sargedas De Sousa[57b,57a], J. V. Da Fonseca Pinto[83b], C. Da Via[101], W. Dabrowski[86a], T. Dado[49], S. Dahbi[33g], T. Dai[106], D. Dal Santo[19], C. Dallapiccola[103], M. Dam[42], G. D'amen[29], V. D'Amico[109], J. Damp[100], J. R. Dandoy[128], M. F. Daneri[30], M. Danninger[142], V. Dao[36], G. Darbo[57b], S. Darmora[6], S. J. Das[29,ai], S. D'Auria[71a,71b], C. David[156b], T. Davidek[133], B. Davis-Purcell[34], I. Dawson[94], H. A. Day-hall[132], K. De[8], R. De Asmundis[72a], N. De Biase[48], S. De Castro[23a,23b], N. De Groot[113], P. de Jong[114], H. De la Torre[115], A. De Maria[14c], A. De Salvo[75a], U. De Sanctis[76a,76b], A. De Santo[146], J. B. De Vivie De Regie[60], D. V. Dedovich[38], J. Degens[114], A. M. Deiana[44], F. Del Corso[23a,23b], J. Del Peso[99], F. Del Rio[63a], F. Deliot[135], C. M. Delitzsch[49], M. Della Pietra[72a,72b], D. Della Volpe[56], A. Dell'Acqua[36], L. Dell'Asta[71a,71b], M. Delmastro[4], P. A. Delsart[60], S. Demers[172], M. Demichev[38], S. P. Denisov[37], L. D'Eramo[40], D. Derendarz[87], F. Derue[127], P. Dervan[92], K. Desch[24], C. Deutsch[24], F. A. Di Bello[57a,57b], A. Di Ciaccio[76a,76b], L. Di Ciaccio[4], A. Di Domenico[75a,75b], C. Di Donato[72a,72b], A. Di Girolamo[36], G. Di Gregorio[36], A. Di Luca[78a,78b], B. Di Micco[77a,77b], R. Di Nardo[77a,77b], C. Diaconu[102], M. Diamantopoulou[34], F. A. Dias[114], T. Dias Do Vale[142], M. A. Diaz[137a,137b], F. G. Diaz Capriles[24], M. Didenko[163], E. B. Diehl[106], L. Diehl[54], S. Díez Cornell[48], C. Diez Pardos[141], C. Dimitriadi[24,161], A. Dimitrievska[17a], J. Dingfelder[24], I-M. Dinu[27b], S. J. Dittmeier[63b], F. Dittus[36], F. Djama[102], T. Djobava[149b], J. I. Djuvsland[16], C. Doglioni[98,101], A. Dohnalova[28a], J. Dolejsi[133], Z. Dolezal[133], K. M. Dona[39], M. Donadelli[83c], B. Dong[107], J. Donini[40], A. D'Onofrio[77a,77b], M. D'Onofrio[92], J. Dopke[134], A. Doria[72a], N. Dos Santos Fernandes[130a], P. Dougan[101], M. T. Dova[90], A. T. Doyle[59], M. A. Draguet[126], E. Dreyer[169], I. Drivas-koulouris[10], M. Drnevich[117], A. S. Drobac[158], M. Drozdova[56], D. Du[62a], T. A. du Pree[114], F. Dubinin[37], M. Dubovsky[28a], E. Duchovni[169], G. Duckeck[109],

O. A. Ducu[27b], D. Duda[52], A. Dudarev[36], E. R. Duden[26], M. D'uffizi[101], L. Duflot[66], M. Dührssen[36], C. Dülsen[171], A. E. Dumitriu[27b], M. Dunford[63a], S. Dungs[49], K. Dunne[47a,47b], A. Duperrin[102], H. Duran Yildiz[3a], M. Düren[58], A. Durglishvili[149b], B. L. Dwyer[115], G. I. Dyckes[17a], M. Dyndal[86a], B. S. Dziedzic[87], Z. O. Earnshaw[146], G. H. Eberwein[126], B. Eckerova[28a], S. Eggebrecht[55], E. Egidio Purcino De Souza[127], L. F. Ehrke[56], G. Eigen[16], K. Einsweiler[17a], T. Ekelof[161], P. A. Ekman[98], S. El Farkh[35b], Y. El Ghazali[35b], H. El Jarrari[35e,148], A. El Moussaouy[108], V. Ellajosyula[161], M. Ellert[161], F. Ellinghaus[171], N. Ellis[36], J. Elmsheuser[29], M. Elsing[36], D. Emeliyanov[134], Y. Enari[153], I. Ene[17a], S. Epari[13], J. Erdmann[49], P. A. Erland[87], M. Errenst[171], M. Escalier[66], C. Escobar[163], E. Etzion[151], G. Evans[130a], H. Evans[68], L. S. Evans[95], M. O. Evans[146], A. Ezhilov[37], S. Ezzarqtouni[35a], F. Fabbri[59], L. Fabbri[23b,23a], G. Facini[96], V. Fadeyev[136], R. M. Fakhrutdinov[37], S. Falciano[75a], L. F. Falda Ulhoa Coelho[36], P. J. Falke[24], J. Faltova[133], C. Fan[162], Y. Fan[14a], Y. Fang[14a,14e], M. Fanti[71a,71b], M. Faraj[69a,69b], Z. Farazpay[97], A. Farbin[8], A. Farilla[77a], T. Farooque[107], S. M. Farrington[52], F. Fassi[35e], D. Fassouliotis[9], M. Faucci Giannelli[76a,76b], W. J. Fawcett[32], L. Fayard[66], P. Federic[133], P. Federicova[131], O. L. Fedin[37,a], G. Fedotov[37], M. Feickert[170], L. Feligioni[102], D. E. Fellers[123], C. Feng[62b], M. Feng[14b], Z. Feng[114], M. J. Fenton[160], A. B. Fenyuk[37], L. Ferencz[48], R. A. M. Ferguson[91], S. I. Fernandez Luengo[137f], P. Fernandez Martinez[13], M. J. V. Fernoux[102], J. Ferrando[48], A. Ferrari[161], P. Ferrari[113,114], R. Ferrari[73a], D. Ferrere[56], C. Ferretti[106], F. Fiedler[100], P. Fiedler[132], A. Filipčič[93], E. K. Filmer[1], F. Filthaut[113], M. C. N. Fiolhais[130a,130c,c], L. Fiorini[163], W. C. Fisher[107], T. Fitschen[101], P. M. Fitzhugh[135], I. Fleck[141], P. Fleischmann[106], T. Flick[171], M. Flores[33d,ac], L. R. Flores Castillo[64a], L. Flores Sanz De Acedo[36], F. M. Follega[78a,78b], N. Fomin[16], J. H. Foo[155], B. C. Forland[68], A. Formica[135], A.C. Forti[101], E. Fortin[36], A. W. Fortman[61], M. G. Foti[17a], L. Fountas[9,j], D. Fournier[66], H. Fox[91], P. Francavilla[74a,74b], S. Francescato[61], S. Franchellucci[56], M. Franchini[23a,23b], S. Franchino[63a], D. Francis[36], L. Franco[113], V. Franco Lima[36], L. Franconi[48], M. Franklin[61], G. Frattari[26], A. C. Freegard[94], W. S. Freund[83b], Y. Y. Frid[151], J. Friend[59], N. Fritzsche[50], A. Froch[54], D. Froidevaux[36], J. A. Frost[126], Y. Fu[62a], S. Fuenzalida Garrido[137f], M. Fujimoto[102], E. Fullana Torregrosa[163,*], K. Y. Fung[64a], E. Furtado De Simas Filho[83b], M. Furukawa[153], J. Fuster[163], A. Gabrielli[23a,23b], A. Gabrielli[155], P. Gadow[36], G. Gagliardi[57a,57b], L. G. Gagnon[17a], E. J. Gallas[126], B. J. Gallop[134], K. K. Gan[119], S. Ganguly[153], Y. Gao[52], F. M. Garay Walls[137a,137b], B. Garcia[29], C. García[163], A. Garcia Alonso[114], A. G. Garcia Caffaro[172], J. E. García Navarro[163], M. Garcia-Sciveres[17a], G. L. Gardner[128], R. W. Gardner[39], N. Garelli[158], D. Garg[80], R. B. Garg[143,n], J. M. Gargan[52], C. A. Garner[155], C. M. Garvey[33a], P. Gaspar[83b], V. K. Gassmann[158], G. Gaudio[73a], V. Gautam[13], P. Gauzzi[75a,75b], I. L. Gavrilenko[37], A. Gavrilyuk[37], C. Gay[164], G. Gaycken[48], E. N. Gazis[10], A. A. Geanta[27b], C. M. Gee[136], C. Gemme[57b], M. H. Genest[60], S. Gentile[75a,75b], A. D. Gentry[112], S. George[95], W. F. George[20], T. Geralis[46], P. Gessinger-Befurt[36], M. E. Geyik[171], M. Ghani[167], M. Ghneimat[141], K. Ghorbanian[94], A. Ghosal[141], A. Ghosh[160], A. Ghosh[7], B. Giacobbe[23b], S. Giagu[75a,75b], T. Giani[114], P. Giannetti[74a], A. Giannini[62a], S. M. Gibson[95], M. Gignac[136], D. T. Gil[86b], A. K. Gilbert[86a], B. J. Gilbert[41], D. Gillberg[34], G. Gilles[114], N. E. K. Gillwald[48], L. Ginabat[127], D. M. Gingrich[2,af], M. P. Giordani[69a,69c], P. F. Giraud[135], G. Giugliarelli[69a,69c], D. Giugni[71a], F. Giuli[36], I. Gkialas[9,j], L. K. Gladilin[37], C. Glasman[99], G. R. Gledhill[123], G. Glemža[48], M. Glisic[123], I. Gnesi[43b,f], Y. Go[29,ai], M. Goblirsch-Kolb[36], B. Gocke[49], D. Godin[108], B. Gokturk[21a], S. Goldfarb[105], T. Golling[56], M. G. D. Gololo[33g], D. Golubkov[37], J. P. Gombas[107], A. Gomes[130a,130b], G. Gomes Da Silva[141], A. J. Gomez Delegido[163], R. Gonçalo[130a,130c], G. Gonella[123], L. Gonella[20], A. Gongadze[149c], F. Gonnella[20], J. L. Gonski[41], R. Y. González Andana[52], S. González de la Hoz[163], S. Gonzalez Fernandez[13], R. Gonzalez Lopez[92], C. Gonzalez Renteria[17a], M. V. Gonzalez Rodrigues[48], R. Gonzalez Suarez[161], S. Gonzalez-Sevilla[56], G. R. Gonzalvo Rodriguez[163], L. Goossens[36], B. Gorini[36], E. Gorini[70a,70b], A. Gorišek[93], T. C. Gosart[128], A. T. Goshaw[51], M. I. Gostkin[38], S. Goswami[121], C. A. Gottardo[36], S. A. Gotz[109], M. Gouighri[35b], V. Goumarre[48], A. G. Goussiou[138], N. Govender[33c], I. Grabowska-Bold[86a], K. Graham[34], E. Gramstad[125], S. Grancagnolo[70a,70b], M. Grandi[146], C. M. Grant[1,135], P. M. Gravila[27f], F. G. Gravili[70a,70b], H. M. Gray[17a], M. Greco[70a,70b], C. Grefe[24], I. M. Gregor[48], P. Grenier[143], S. G. Grewe[110], C. Grieco[13], A. A. Grillo[136], K. Grimm[31], S. Grinstein[13,s], J.-F. Grivaz[66], E. Gross[169], J. Grosse-Knetter[55], C. Grud[106], J. C. Grundy[126], L. Guan[106], W. Guan[29], C. Gubbels[164], J. G. R. Guerrero Rojas[163], G. Guerrieri[69a,69c], F. Guescini[110], R. Gugel[100], J. A. M. Guhit[106], A. Guida[18], T. Guillemin[4], E. Guilloton[134,167], S. Guindon[36], F. Guo[14a,14e], J. Guo[62c], L. Guo[48], Y. Guo[106], R. Gupta[48], R. Gupta[129], S. Gurbuz[24], S. S. Gurdasani[54], G. Gustavino[36], M. Guth[56], P. Gutierrez[120], L. F. Gutierrez Zagazeta[128], M. Gutsche[50], C. Gutschow[96], C. Gwenlan[126], C. B. Gwilliam[92], E. S. Haaland[125], A. Haas[117], M. Habedank[48], C. Haber[17a], H. K. Hadavand[8], A. Hadef[100], S. Hadzic[110], A. I. Hagan[91], J. J. Hahn[141], E. H. Haines[96], M. Haleem[166], J. Haley[121], J. J. Hall[139], G. D. Hallewell[102], L. Halser[19], K.

Hamano[165], M. Hamer[24], G. N. Hamity[52], E. J. Hampshire[95], J. Han[62b], K. Han[62a], L. Han[14c], L. Han[62a], S. Han[17a], Y. F. Han[155], K. Hanagaki[84], M. Hance[136], D. A. Hangal[41,ab], H. Hanif[142], M. D. Hank[128], R. Hankache[101], J. B. Hansen[42], J. D. Hansen[42], P. H. Hansen[42], K. Hara[157], D. Harada[56], T. Harenberg[171], S. Harkusha[37], M. L. Harris[103], Y. T. Harris[126], J. Harrison[13], N. M. Harrison[119], P. F. Harrison[167], N. M. Hartman[110], N. M. Hartmann[109], Y. Hasegawa[140], R. Hauser[107], C. M. Hawkes[20], R. J. Hawkings[36], Y. Hayashi[153], S. Hayashida[111], D. Hayden[107], C. Hayes[106], R. L. Hayes[114], C. P. Hays[126], J. M. Hays[94], H. S. Hayward[92], F. He[62a], M. He[14a,14e], Y. He[154], Y. He[48], N. B. Heatley[94], V. Hedberg[98], A. L. Heggelund[125], N. D. Hehir[94,*], C. Heidegger[54], K. K. Heidegger[54], W. D. Heidorn[81], J. Heilman[34], S. Heim[48], T. Heim[17a], J. G. Heinlein[128], J. J. Heinrich[123], L. Heinrich[110,ad], J. Hejbal[131], L. Helary[48], A. Held[170], S. Hellesund[16], C. M. Helling[164], S. Hellman[47a,47b], R. C. W. Henderson[91], L. Henkelmann[32], A. M. Henriques Correia[36], H. Herde[98], Y. Hernández Jiménez[145], L. M. Herrmann[24], T. Herrmann[50], G. Herten[54], R. Hertenberger[109], L. Hervas[36], M. E. Hesping[100], N. P. Hessey[156a], H. Hibi[85], E. Hill[155], S. J. Hillier[20], J. R. Hinds[107], F. Hinterkeuser[24], M. Hirose[124], S. Hirose[157], D. Hirschbuehl[171], T. G. Hitchings[101], B. Hiti[93], J. Hobbs[145], R. Hobincu[27e], N. Hod[169], M. C. Hodgkinson[139], B. H. Hodkinson[32], A. Hoecker[36], D. D. Hofer[106], J. Hofer[48], T. Holm[24], M. Holzbock[110], L. B. A. H. Hommels[32], B. P. Honan[101], J. Hong[62c], T. M. Hong[129], B. H. Hooberman[162], W. H. Hopkins[6], Y. Horii[111], S. Hou[148], A. S. Howard[93], J. Howarth[59], J. Hoya[6], M. Hrabovsky[122], A. Hrynevich[48], T. Hryn'ova[4], P. J. Hsu[65], S.-C. Hsu[138], Q. Hu[62a], Y. F. Hu[14a,14e], S. Huang[64b], X. Huang[14c], X. Huang[14a,14e], Y. Huang[139], Y. Huang[14a], Z. Huang[101], Z. Hubacek[132], M. Huebner[24], F. Huegging[24], T. B. Huffman[126], C. A. Hugli[48], M. Huhtinen[36], S. K. Huiberts[16], R. Hulsken[104], N. Huseynov[12], J. Huston[107], J. Huth[61], R. Hyneman[143], G. Iacobucci[56], G. Iakovidis[29], I. Ibragimov[141], L. Iconomidou-Fayard[66], P. Iengo[72a,72b], R. Iguchi[153], T. Iizawa[126], Y. Ikegami[84], N. Ilic[155], H. Imam[35a], M. Ince Lezki[56], T. Ingebretsen Carlson[47a,47b], G. Introzzi[73a,73b], M. Iodice[77a], V. Ippolito[75a,75b], R. K. Irwin[92], M. Ishino[153], W. Islam[170], C. Issever[18,48], S. Istin[21a,ak], H. Ito[168], J. M. Iturbe Ponce[64a], R. Iuppa[78a,78b], A. Ivina[169], J. M. Izen[45], V. Izzo[72a], P. Jacka[131,132], P. Jackson[1], R. M. Jacobs[48], B. P. Jaeger[142], C. S. Jagfeld[109], G. Jain[156a], P. Jain[54], K. Jakobs[54], T. Jakoubek[169], J. Jamieson[59], K. W. Janas[86a], M. Javurkova[103], F. Jeanneau[135], L. Jeanty[123], J. Jejelava[149a,z], P. Jenni[54,g], C. E. Jessiman[34], S. Jézéquel[4], C. Jia[62b], J. Jia[145], X. Jia[61], X. Jia[14a,14e], Z. Jia[14c], S. Jiggins[48], J. Jimenez Pena[13], S. Jin[14c], A. Jinaru[27b], O. Jinnouchi[154], P. Johansson[139], K. A. Johns[7], J. W. Johnson[136], D. M. Jones[32], E. Jones[48], P. Jones[32], R. W. L. Jones[91], T. J. Jones[92], H. L. Joos[36,55], R. Joshi[119], J. Jovicevic[15], X. Ju[17a], J. J. Junggeburth[103], T. Junkermann[63a], A. Juste Rozas[13,s], M. K. Juzek[87], S. Kabana[137e], A. Kaczmarska[87], M. Kado[110], H. Kagan[119], M. Kagan[143], A. Kahn[41], A. Kahn[128], C. Kahra[100], T. Kaji[153], E. Kajomovitz[150], N. Kakati[169], I. Kalaitzidou[54], C. W. Kalderon[29], A. Kamenshchikov[155], N. J. Kang[136], D. Kar[33g], K. Karava[126], M. J. Kareem[156b], E. Karentzos[54], I. Karkanias[152], O. Karkout[114], S. N. Karpov[38], Z. M. Karpova[38], V. Kartvelishvili[91], A. N. Karyukhin[37], E. Kasimi[152], J. Katzy[48], S. Kaur[34], K. Kawade[140], M. P. Kawale[120], C. Kawamoto[88], T. Kawamoto[135], E. F. Kay[36], F. I. Kaya[158], S. Kazakos[107], V. F. Kazanin[37], Y. Ke[145], J. M. Keaveney[33a], R. Keeler[165], G. V. Kehris[61], J. S. Keller[34], A. S. Kelly[96], J. J. Kempster[146], K. E. Kennedy[41], P. D. Kennedy[100], O. Kepka[131], B. P. Kerridge[167], S. Kersten[171], B. P. Kerševan[93], S. Keshri[66], L. Keszeghova[28a], S. Ketabchi Haghighat[155], R. A. Khan[129], M. Khandoga[127], A. Khanov[121], A. G. Kharlamov[37], T. Kharlamova[37], E. E. Khoda[138], M. Kholodenko[37], T. J. Khoo[18], G. Khoriauli[166], J. Khubua[149b], Y. A. R. Khwaira[66], A. Kilgallon[123], D. W. Kim[47a,47b], Y. K. Kim[39], N. Kimura[96], M. K. Kingston[55], A. Kirchhoff[55], C. Kirfel[24], F. Kirfel[24], J. Kirk[134], A. E. Kiryunin[110], C. Kitsaki[10], O. Kivernyk[24], M. Klassen[63a], C. Klein[34], L. Klein[166], M. H. Klein[106], M. Klein[92], S. B. Klein[56], U. Klein[92], P. Klimek[36], A. Klimentov[29], T. Klioutchnikova[36], P. Kluit[114], S. Kluth[110], E. Kneringer[79], T. M. Knight[155], A. Knue[49], R. Kobayashi[88], D. Kobylianskii[169], S. F. Koch[126], M. Kocian[143], P. Kodyš[133], D. M. Koeck[123], P. T. Koenig[24], T. Koffas[34], O. Kolay[50], M. Kolb[135], I. Koletsou[4], T. Komarek[122], K. Köneke[54], A. X. Y. Kong[1], T. Kono[118], N. Konstantinidis[96], P. Kontaxakis[56], B. Konya[98], R. Kopeliansky[68], S. Koperny[86a], K. Korcyl[87], K. Kordas[152,e], G. Koren[151], A. Korn[96], S. Korn[55], I. Korolkov[13], N. Korotkova[37], B. Kortman[114], O. Kortner[110], S. Kortner[110], W. H. Kostecka[115], V. V. Kostyukhin[141], A. Kotsokechagia[135], A. Kotwal[51], A. Koulouris[36], A. Kourkoumeli-Charalampidi[73a,73b], C. Kourkoumelis[9], E. Kourlitis[110,ad], O. Kovanda[146], R. Kowalewski[165], W. Kozanecki[135], A. S. Kozhin[37], V. A. Kramarenko[37], G. Kramberger[93], P. Kramer[100], M. W. Krasny[127], A. Krasznahorkay[36], J. W. Kraus[171], J. A. Kremer[48], T. Kresse[50], J. Kretzschmar[92], K. Kreul[18], P. Krieger[155], S. Krishnamurthy[103], M. Krivos[133], K. Krizka[20], K. Kroeninger[49], H. Kroha[110], J. Kroll[131], J. Kroll[128], K. S. Krowpman[107], U. Kruchonak[38], H. Krüger[24], N. Krumnack[81], M. C. Kruse[51], J. A. Krzysiak[87], O. Kuchinskaia[37], S. Kuday[3a], S. Kuehn[36], R. Kuesters[54], T. Kuhl[48], V. Kukhtin[38], Y. Kulchitsky[37,a], S.

Kuleshov[137b,137d], M. Kumar[33g], N. Kumari[48], A. Kupco[131], T. Kupfer[49], A. Kupich[37], O. Kuprash[54], H. Kurashige[85], L. L. Kurchaninov[156a], O. Kurdysh[66], Y. A. Kurochkin[37], A. Kurova[37], M. Kuze[154], A. K. Kvam[103], J. Kvita[122], T. Kwan[104], N. G. Kyriacou[106], L. A. O. Laatu[102], C. Lacasta[163], F. Lacava[75a,75b], H. Lacker[18], D. Lacour[127], N. N. Lad[96], E. Ladygin[38], B. Laforge[127], T. Lagouri[137e], F. Z. Lahbabi[35a], S. Lai[55], I. K. Lakomiec[86a], N. Lalloue[60], J. E. Lambert[165], S. Lammers[68], W. Lampl[7], C. Lampoudis[152,e], A. N. Lancaster[115], E. Lançon[29], U. Landgraf[54], M. P. J. Landon[94], V. S. Lang[54], R. J. Langenberg[103], O. K. B. Langrekken[125], A. J. Lankford[160], F. Lanni[36], K. Lantzsch[24], A. Lanza[73a], A. Lapertosa[57a,57b], J. F. Laporte[135], T. Lari[71a], F. Lasagni Manghi[23b], M. Lassnig[36], V. Latonova[131], A. Laudrain[100], A. Laurier[150], S. D. Lawlor[139], Z. Lawrence[101], R. Lazaridou[167], M. Lazzaroni[71a,71b], B. Le[101], E. M. Le Boulicaut[51], B. Leban[93], A. Lebedev[81], M. LeBlanc[101], F. Ledroit-Guillon[60], A. C. A. Lee[96], S. C. Lee[148], S. Lee[47a,47b], T. F. Lee[92], L. L. Leeuw[33c], H. P. Lefebvre[95], M. Lefebvre[165], C. Leggett[17a], G. Lehmann Miotto[36], M. Leigh[56], W. A. Leight[103], W. Leinonen[113], A. Leisos[152,r], M. A. L. Leite[83c], C. E. Leitgeb[48], R. Leitner[133], K. J. C. Leney[44], T. Lenz[24], S. Leone[74a], C. Leonidopoulos[52], A. Leopold[144], C. Leroy[108], R. Les[107], C. G. Lester[32], M. Levchenko[37], J. Levêque[4], D. Levin[106], L. J. Levinson[169], M. P. Lewicki[87], D. J. Lewis[4], A. Li[5], B. Li[62b], C. Li[62a], C-Q. Li[62c], H. Li[62a], H. Li[62b], H. Li[14c], H. Li[14b], H. Li[62b], J. Li[62c], K. Li[138], L. Li[62c], M. Li[14a,14e], Q. Y. Li[62a], S. Li[14a,14e], S. Li[62d,62c,d], T. Li[5], X. Li[104], Z. Li[126], Z. Li[104], Z. Li[92], Z. Li[14a,14e], S. Liang[14a,14e], Z. Liang[14a], M. Liberatore[135], B. Liberti[76a], K. Lie[64c], J. Lieber Marin[83b], H. Lien[68], K. Lin[107], R. E. Lindley[7], J. H. Lindon[2], E. Lipeles[128], A. Lipniacka[16], A. Lister[164], J. D. Little[4], B. Liu[14a], B. X. Liu[142], D. Liu[62d,62c], J. B. Liu[62a], J. K. K. Liu[32], K. Liu[62d,62c], M. Liu[62a], M. Y. Liu[62a], P. Liu[14a], Q. Liu[62c,62d,138], X. Liu[62a], Y. Liu[14d,14e], Y. L. Liu[62b], Y. W. Liu[62a], J. Llorente Merino[142], S. L. Lloyd[94], E. M. Lobodzinska[48], P. Loch[7], T. Lohse[18], K. Lohwasser[139], E. Loiacono[48], M. Lokajicek[131,*], J. D. Lomas[20], J. D. Long[162], I. Longarini[160], L. Longo[70a,70b], R. Longo[162], I. Lopez Paz[67], A. Lopez Solis[48], J. Lorenz[109], N. Lorenzo Martinez[4], A. M. Lory[109], G. Löschcke Centeno[146], O. Loseva[37], X. Lou[47a,47b], X. Lou[14a,14e], A. Lounis[66], J. Love[6], P. A. Love[91], G. Lu[14a,14e], M. Lu[80], S. Lu[128], Y. J. Lu[65], H. J. Lubatti[138], C. Luci[75a,75b], F. L. Lucio Alves[14c], A. Lucotte[60], F. Luehring[68], I. Luise[145], O. Lukianchuk[66], O. Lundberg[144], B. Lund-Jensen[144], N. A. Luongo[123], M. S. Lutz[151], A. B. Lux[25], D. Lynn[29], H. Lyons[92], R. Lysak[131], E. Lytken[98], V. Lyubushkin[38], T. Lyubushkina[38], M. M. Lyukova[145], H. Ma[29], K. Ma[62a], L. L. Ma[62b], W. Ma[62a], Y. Ma[121], D. M. Mac Donell[165], G. Maccarrone[53], J. C. MacDonald[100], P. C. Machado De Abreu Farias[83b], R. Madar[40], W. F. Mader[50], T. Madula[96], J. Maeda[85], T. Maeno[29], H. Maguire[139], V. Maiboroda[135], A. Maio[130a,130b,130d], K. Maj[86a], O. Majersky[48], S. Majewski[123], N. Makovec[66], V. Maksimovic[15], B. Malaescu[127], Pa. Malecki[87], V. P. Maleev[37], F. Malek[60], M. Mali[93], D. Malito[95], U. Mallik[80], S. Maltezos[10], S. Malyukov[38], J. Mamuzic[13], G. Mancini[53], G. Manco[73a,73b], J. P. Mandalia[94], I. Mandić[93], L. Manhaes de Andrade Filho[83a], I. M. Maniatis[169], J. Manjarres Ramos[102,aa], D. C. Mankad[169], A. Mann[109], B. Mansoulie[135], S. Manzoni[36], X. Mapekula[33c], A. Marantis[152,r], G. Marchiori[5], M. Marcisovsky[131], C. Marcon[71a], M. Marinescu[20], M. Marjanovic[120], E. J. Marshall[91], Z. Marshall[17a], S. Marti-Garcia[163], T. A. Martin[167], V. J. Martin[52], B. Martin dit Latour[16], L. Martinelli[75a,75b], M. Martinez[13,s], P. Martinez Agullo[163], V. I. Martinez Outschoorn[103], P. Martinez Suarez[13], S. Martin-Haugh[134], V. S. Martoiu[27b], A. C. Martyniuk[96], A. Marzin[36], D. Mascione[78a,78b], L. Masetti[100], T. Mashimo[153], J. Masik[101], A. L. Maslennikov[37], L. Massa[23b], P. Massarotti[72a,72b], P. Mastrandrea[74a,74b], A. Mastroberardino[43a,43b], T. Masubuchi[153], T. Mathisen[161], J. Matousek[133], N. Matsuzawa[153], J. Maurer[27b], B. Maček[93], D. A. Maximov[37], R. Mazini[148], I. Maznas[152], M. Mazza[107], S. M. Mazza[136], E. Mazzeo[71a,71b], C. Mc Ginn[29], J. P. Mc Gowan[104], S. P. Mc Kee[106], E. F. McDonald[105], A. E. McDougall[114], J. A. Mcfayden[146], R. P. McGovern[128], G. Mchedlidze[149b], R. P. Mckenzie[33g], T. C. Mclachlan[48], D. J. Mclaughlin[96], S. J. McMahon[134], C. M. Mcpartland[92], R. A. McPherson[165,w], S. Mehlhase[109], A. Mehta[92], D. Melini[150], B. R. Mellado Garcia[33g], A. H. Melo[55], F. Meloni[48], A. M. Mendes Jacques Da Costa[101], H. Y. Meng[155], L. Meng[91], S. Menke[110], M. Mentink[36], E. Meoni[43a,43b], G. Mercado[115], C. Merlassino[126], L. Merola[72a,72b], C. Meroni[71a,71b], G. Merz[106], O. Meshkov[37], J. Metcalfe[6], A. S. Mete[6], C. Meyer[68], J-P. Meyer[135], R. P. Middleton[134], L. Mijović[52], G. Mikenberg[169], M. Mikestikova[131], M. Mikuž[93], H. Mildner[100], A. Milic[36], C. D. Milke[44], D. W. Miller[39], L. S. Miller[34], A. Milov[169], D. A. Milstead[47a,47b], T. Min[14c], A. A. Minaenko[37], I. A. Minashvili[149b], L. Mince[59], A. I. Mincer[117], B. Mindur[86a], M. Mineev[38], Y. Mino[88], L. M. Mir[13], M. Miralles Lopez[163], M. Mironova[17a], A. Mishima[153], M. C. Missio[113], A. Mitra[167], V. A. Mitsou[163], Y. Mitsumori[111], O. Miu[155], P. S. Miyagawa[94], T. Mkrtchyan[63a], M. Mlinarevic[96], T. Mlinarevic[96], M. Mlynarikova[36], S. Mobius[19], P. Moder[48], P. Mogg[109], A. F. Mohammed[14a,14e], S. Mohapatra[41], G. Mokgatitswane[33g], L. Moleri[169], B. Mondal[141], S. Mondal[132], K. Mönig[48], E. Monnier[102], L. Monsonis Romero[163], J. Montejo Berlingen[13], M. Montella[119], F. Montereali[77a,77b], F.

Monticelli[90], S. Monzani[69a,69c], N. Morange[66], A. L. Moreira De Carvalho[130a], M. Moreno Llácer[163], C. Moreno Martinez[56], P. Morettini[57b], S. Morgenstern[36], M. Morii[61], M. Morinaga[153], A. K. Morley[36], F. Morodei[75a,75b], L. Morvaj[36], P. Moschovakos[36], B. Moser[36], M. Mosidze[149b], T. Moskalets[54], P. Moskvitina[113], J. Moss[31,l], E. J. W. Moyse[103], O. Mtintsilana[33g], S. Muanza[102], J. Mueller[129], D. Muenstermann[91], R. Müller[19], G. A. Mullier[161], A. J. Mullin[32], J. J. Mullin[128], D. P. Mungo[155], D. Munoz Perez[163], F. J. Munoz Sanchez[101], M. Murin[101], W. J. Murray[167,134], A. Murrone[71a,71b], M. Muškinja[17a], C. Mwewa[29], A. G. Myagkov[37,a], A. J. Myers[8], G. Myers[68], M. Myska[132], B. P. Nachman[17a], O. Nackenhorst[49], A. Nag[50], K. Nagai[126], K. Nagano[84], J. L. Nagle[29,ai], E. Nagy[102], A. M. Nairz[36], Y. Nakahama[84], K. Nakamura[84], K. Nakkalil[5], H. Nanjo[124], R. Narayan[44], E. A. Narayanan[112], I. Naryshkin[37], M. Naseri[34], S. Nasri[159], C. Nass[24], G. Navarro[22a], J. Navarro-Gonzalez[163], R. Nayak[151], A. Nayaz[18], P. Y. Nechaeva[37], F. Nechansky[48], L. Nedic[126], T. J. Neep[20], A. Negri[73a,73b], M. Negrini[23b], C. Nellist[114], C. Nelson[104], K. Nelson[106], S. Nemecek[131], M. Nessi[36,h], M. S. Neubauer[162], F. Neuhaus[100], J. Neundorf[48], R. Newhouse[164], P. R. Newman[20], C. W. Ng[129], Y. W. Y. Ng[48], B. Ngair[35e], H. D. N. Nguyen[108], R. B. Nickerson[126], R. Nicolaidou[135], J. Nielsen[136], M. Niemeyer[55], J. Niermann[36,55], N. Nikiforou[36], V. Nikolaenko[37,a], I. Nikolic-Audit[127], K. Nikolopoulos[20], P. Nilsson[29], I. Ninca[48], H. R. Nindhito[56], G. Ninio[151], A. Nisati[75a], N. Nishu[2], R. Nisius[110], J-E. Nitschke[50], E. K. Nkadimeng[33g], T. Nobe[153], D. L. Noel[32], T. Nommensen[147], M. B. Norfolk[139], R. R. B. Norisam[96], B. J. Norman[34], J. Novak[93], T. Novak[48], L. Novotny[132], R. Novotny[112], L. Nozka[122], K. Ntekas[160], N. M. J. Nunes De Moura Junior[83b], E. Nurse[96], J. Ocariz[127], A. Ochi[85], I. Ochoa[130a], S. Oerdek[48,t], J. T. Offermann[39], A. Ogrodnik[133], A. Oh[101], C. C. Ohm[144], H. Oide[84], R. Oishi[153], M. L. Ojeda[48], M. W. O'Keefe[92], Y. Okumura[153], L. F. Oleiro Seabra[130a], S. A. Olivares Pino[137d], D. Oliveira Damazio[29], D. Oliveira Goncalves[83a], J. L. Oliver[160], Ö. O. Öncel[54], A.P. O'Neill[19], A. Onofre[130a,130e], P. U. E. Onyisi[11], M. J. Oreglia[39], G. E. Orellana[90], D. Orestano[77a,77b], N. Orlando[13], R. S. Orr[155], V. O'Shea[59], L. M. Osojnak[128], R. Ospanov[62a], G. Otero y Garzon[30], H. Otono[89], P. S. Ott[63a], G. J. Ottino[17a], M. Ouchrif[35d], J. Ouellette[29], F. Ould-Saada[125], M. Owen[59], R. E. Owen[134], K. Y. Oyulmaz[21a], V. E. Ozcan[21a], F. Ozturk[87], N. Ozturk[8], S. Ozturk[82], H. A. Pacey[126], A. Pacheco Pages[13], C. Padilla Aranda[13], G. Padovano[75a,75b], S. Pagan Griso[17a], G. Palacino[68], A. Palazzo[70a,70b], S. Palestini[36], J. Pan[172], T. Pan[64a], D. K. Panchal[11], C. E. Pandini[114], J. G. Panduro Vazquez[95], H. D. Pandya[1], H. Pang[14b], P. Pani[48], G. Panizzo[69a,69c], L. Paolozzi[56], C. Papadatos[108], S. Parajuli[44], A. Paramonov[6], C. Paraskevopoulos[10], D. Paredes Hernandez[64b], K. R. Park[41], T. H. Park[155], M. A. Parker[32], F. Parodi[57b,57a], E. W. Parrish[115], V. A. Parrish[52], J. A. Parsons[41], U. Parzefall[54], B. Pascual Dias[108], L. Pascual Dominguez[151], E. Pasqualucci[75a], S. Passaggio[57b], F. Pastore[95], P. Pasuwan[47a,47b], P. Patel[87], U. M. Patel[51], J. R. Pater[101], T. Pauly[36], J. Pearkes[143], M. Pedersen[125], R. Pedro[130a], S. V. Peleganchuk[37], O. Penc[36], E. A. Pender[52], K. E. Penski[109], M. Penzin[37], B. S. Peralva[83d], A. P. Pereira Peixoto[60], L. Pereira Sanchez[47a,47b], D. V. Perepelitsa[29,ai], E. Perez Codina[156a], M. Perganti[10], L. Perini[71a,71b,*], H. Pernegger[36], O. Perrin[40], K. Peters[48], R. F. Y. Peters[101], B. A. Petersen[36], T. C. Petersen[42], E. Petit[102], V. Petousis[132], C. Petridou[152,e], A. Petrukhin[141], M. Pettee[17a], N. E. Pettersson[36], A. Petukhov[37], K. Petukhova[133], R. Pezoa[137f], L. Pezzotti[36], G. Pezzullo[172], T. M. Pham[170], T. Pham[105], P. W. Phillips[134], G. Piacquadio[145], E. Pianori[17a], F. Piazza[123], R. Piegaia[30], D. Pietreanu[27b], A. D. Pilkington[101], M. Pinamonti[69a,69c], J. L. Pinfold[2], B. C. Pinheiro Pereira[130a], A. E. Pinto Pinoargote[100,135], L. Pintucci[69a,69c], K. M. Piper[146], A. Pirttikoski[56], D. A. Pizzi[34], L. Pizzimento[64b], A. Pizzini[114], M.-A. Pleier[29], V. Plesanovs[54], V. Pleskot[133], E. Plotnikova[38], G. Poddar[4], R. Poettgen[98], L. Poggioli[127], I. Pokharel[55], S. Polacek[133], G. Polesello[73a], A. Poley[142,156a], R. Polifka[132], A. Polini[23b], C. S. Pollard[167], Z. B. Pollock[119], V. Polychronakos[29], E. Pompa Pacchi[75a,75b], D. Ponomarenko[113], L. Pontecorvo[36], S. Popa[27a], G. A. Popeneciu[27d], A. Poreba[36], D. M. Portillo Quintero[156a], S. Pospisil[132], M. A. Postill[139], P. Postolache[27c], K. Potamianos[167], P. A. Potepa[86a], I. N. Potrap[38], C. J. Potter[32], H. Potti[1], T. Poulsen[48], J. Poveda[163], M. E. Pozo Astigarraga[36], A. Prades Ibanez[163], J. Pretel[54], D. Price[101], M. Primavera[70a], M. A. Principe Martin[99], R. Privara[122], T. Procter[59], M. L. Proffitt[138], N. Proklova[128], K. Prokofiev[64c], G. Proto[110], S. Protopopescu[29], J. Proudfoot[6], M. Przybycien[86a], W. W. Przygoda[86b], J. E. Puddefoot[139], D. Pudzha[37], D. Pyatiizbyantseva[37], J. Qian[106], D. Qichen[101], Y. Qin[101], T. Qiu[52], A. Quadt[55], M. Queitsch-Maitland[101], G. Quetant[56], R. P. Quinn[164], G. Rabanal Bolanos[61], D. Rafanoharana[54], F. Ragusa[71a,71b], J. L. Rainbolt[39], J. A. Raine[56], S. Rajagopalan[29], E. Ramakoti[37], I. A. Ramirez-Berend[34], K. Ran[14e,48], N. P. Rapheeha[33g], H. Rasheed[27b], V. Raskina[127], D. F. Rassloff[63a], S. Rave[100], B. Ravina[55], I. Ravinovich[169], M. Raymond[36], A. L. Read[125], N. P. Readioff[139], D. M. Rebuzzi[73a,73b], G. Redlinger[29], A. S. Reed[110], K. Reeves[26], J. A. Reidelsturz[171], D. Reikher[151], A. Rej[49], C. Rembser[36], A. Renardi[48], M. Renda[27b], M. B. Rendel[110], F. Renner[48], A. G. Rennie[160], A. L. Rescia[48], S. Resconi[71a], M. Ressegotti[57a,57b], S.

Rettie[36], J. G. Reyes Rivera[107], E. Reynolds[17a], O. L. Rezanova[37], P. Reznicek[133], N. Ribaric[91], E. Ricci[78a,78b], R. Richter[110], S. Richter[47a,47b], E. Richter-Was[86b], M. Ridel[127], S. Ridouani[35d], P. Rieck[117], P. Riedler[36], E. M. Riefel[47a,47b], J. O. Rieger[114], M. Rijssenbeek[145], A. Rimoldi[73a,73b], M. Rimoldi[36], L. Rinaldi[23b,23a], T. T. Rinn[29], M. P. Rinnagel[109], G. Ripellino[161], I. Riu[13], P. Rivadeneira[48], J. C. Rivera Vergara[165], F. Rizatdinova[121], E. Rizvi[94], B. A. Roberts[167], B. R. Roberts[17a], S. H. Robertson[104,w], D. Robinson[32], C. M. Robles Gajardo[137f], M. Robles Manzano[100], A. Robson[59], A. Rocchi[76a,76b], C. Roda[74a,74b], S. Rodriguez Bosca[63a], Y. Rodriguez Garcia[22a], A. Rodriguez Rodriguez[54], A. M. Rodríguez Vera[156b], S. Roe[36], J. T. Roemer[160], A. R. Roepe-Gier[136], J. Roggel[171], O. Røhne[125], R. A. Rojas[103], C. P. A. Roland[127], J. Roloff[29], A. Romaniouk[37], E. Romano[73a,73b], M. Romano[23b], A. C. Romero Hernandez[162], N. Rompotis[92], L. Roos[127], S. Rosati[75a], B. J. Rosser[39], E. Rossi[126], E. Rossi[72a,72b], L. P. Rossi[57b], L. Rossini[54], R. Rosten[119], M. Rotaru[27b], B. Rottler[54], C. Rougier[102,aa], D. Rousseau[66], D. Rousso[32], A. Roy[162], S. Roy-Garand[155], A. Rozanov[102], Z. M. A. Rozario[59], Y. Rozen[150], X. Ruan[33g], A. Rubio Jimenez[163], A. J. Ruby[92], V. H. Ruelas Rivera[18], T. A. Ruggeri[1], A. Ruggiero[126], A. Ruiz-Martinez[163], A. Rummler[36], Z. Rurikova[54], N. A. Rusakovich[38], H. L. Russell[165], G. Russo[75a,75b], J. P. Rutherfoord[7], S. Rutherford Colmenares[32], K. Rybacki[91], M. Rybar[133], E. B. Rye[125], A. Ryzhov[44], J. A. Sabater Iglesias[56], P. Sabatini[163], L. Sabetta[75a,75b], H. F-W. Sadrozinski[136], F. Safai Tehrani[75a], B. Safarzadeh Samani[134], M. Safdari[143], S. Saha[165], M. Sahinsoy[110], M. Saimpert[135], M. Saito[153], T. Saito[153], D. Salamani[36], A. Salnikov[143], J. Salt[163], A. Salvador Salas[151], D. Salvatore[43a,43b], F. Salvatore[146], A. Salzburger[36], D. Sammel[54], D. Sampsonidis[152,e], D. Sampsonidou[123], J. Sánchez[163], A. Sanchez Pineda[4], V. Sanchez Sebastian[163], H. Sandaker[125], C. O. Sander[48], J. A. Sandesara[103], M. Sandhoff[171], C. Sandoval[22b], D. P. C. Sankey[134], T. Sano[88], A. Sansoni[53], L. Santi[75a,75b], C. Santoni[40], H. Santos[130a,130b], S. N. Santpur[17a], A. Santra[169], K. A. Saoucha[116b], J. G. Saraiva[130a,130d], J. Sardain[7], O. Sasaki[84], K. Sato[157], C. Sauer[63b], F. Sauerburger[54], E. Sauvan[4], P. Savard[155,af], R. Sawada[153], C. Sawyer[134], L. Sawyer[97], I. Sayago Galvan[163], C. Sbarra[23b], A. Sbrizzi[23a,23b], T. Scanlon[96], J. Schaarschmidt[138], P. Schacht[110], U. Schäfer[100], A. C. Schaffer[44,66], D. Schaile[109], R. D. Schamberger[145], C. Scharf[18], M. M. Schefer[19], V. A. Schegelsky[37], D. Scheirich[133], F. Schenck[18], M. Schernau[160], C. Scheulen[55], C. Schiavi[57a,57b], E. J. Schioppa[70a,70b], M. Schioppa[43b,43a], B. Schlag[143,n], K. E. Schleicher[54], S. Schlenker[36], J. Schmeing[171], M. A. Schmidt[171], K. Schmieden[100], C. Schmitt[100], N. Schmitt[100], S. Schmitt[48], L. Schoeffel[135], A. Schoening[63b], P. G. Scholer[54], E. Schopf[126], M. Schott[100], J. Schovancova[36], S. Schramm[56], F. Schroeder[171], T. Schroer[56], H-C. Schultz-Coulon[63a], M. Schumacher[54], B. A. Schumm[136], Ph. Schune[135], A. J. Schuy[138], H. R. Schwartz[136], A. Schwartzman[143], T. A. Schwarz[106], Ph. Schwemling[135], R. Schwienhorst[107], A. Sciandra[136], G. Sciolla[26], F. Scuri[74a], C. D. Sebastiani[92], K. Sedlaczek[115], P. Seema[18], S. C. Seidel[112], A. Seiden[136], B. D. Seidlitz[41], C. Seitz[48], J. M. Seixas[83b], G. Sekhniaidze[72a], S. J. Sekula[44], L. Selem[60], N. Semprini-Cesari[23b,23a], D. Sengupta[56], V. Senthilkumar[163], L. Serin[66], L. Serkin[69a,69b], M. Sessa[76a,76b], H. Severini[120], F. Sforza[57a,57b], A. Sfyrla[56], E. Shabalina[55], R. Shaheen[144], J. D. Shahinian[128], D. Shaked Renous[169], L. Y. Shan[14a], M. Shapiro[17a], A. Sharma[36], A. S. Sharma[164], P. Sharma[80], S. Sharma[48], P. B. Shatalov[37], K. Shaw[146], S. M. Shaw[101], A. Shcherbakova[37], Q. Shen[62c,5], P. Sherwood[96], L. Shi[96], X. Shi[14a], C. O. Shimmin[172], J. D. Shinner[95], I. P. J. Shipsey[126], S. Shirabe[56,h], M. Shiyakova[38,u], J. Shlomi[169], M. J. Shochet[39], J. Shojaii[105], D. R. Shope[125], B. Shrestha[120], S. Shrestha[119,aj], E. M. Shrif[33g], M. J. Shroff[165], P. Sicho[131], A. M. Sickles[162], E. Sideras Haddad[33g], A. Sidoti[23b], F. Siegert[50], Dj. Sijacki[15], R. Sikora[86a], F. Sili[90], J. M. Silva[20], M. V. Silva Oliveira[29], S. B. Silverstein[47a], S. Simion[66], R. Simoniello[36], E. L. Simpson[59], H. Simpson[146], L. R. Simpson[106], N. D. Simpson[98], S. Simsek[82], S. Sindhu[55], P. Sinervo[155], S. Singh[155], S. Sinha[48], S. Sinha[101], M. Sioli[23b,23a], I. Siral[36], E. Sitnikova[48], S. Yu. Sivoklokov[37,*], J. Sjölin[47a,47b], A. Skaf[55], E. Skorda[20], P. Skubic[120], M. Slawinska[87], V. Smakhtin[169], B. H. Smart[134], J. Smiesko[36], S. Yu. Smirnov[37], Y. Smirnov[37], L. N. Smirnova[37,a], O. Smirnova[98], A. C. Smith[41], E. A. Smith[39], H. A. Smith[126], J. L. Smith[92], R. Smith[143], M. Smizanska[91], K. Smolek[132], A. A. Snesarev[37], S. R. Snider[155], H. L. Snoek[114], S. Snyder[29], R. Sobie[165,w], A. Soffer[151], C. A. Solans Sanchez[36], E. Yu. Soldatov[37], U. Soldevila[163], A. A. Solodkov[37], S. Solomon[26], A. Soloshenko[38], K. Solovieva[54], O. V. Solovyanov[40], V. Solovyev[37], P. Sommer[36], A. Sonay[13], W. Y. Song[156b], J. M. Sonneveld[114], A. Sopczak[132], A. L. Sopio[96], F. Sopkova[28b], I. R. Sotarriva Alvarez[154], V. Sothilingam[63a], O. J. Soto Sandoval[137c,137b], S. Sottocornola[68], R. Soualah[116b], Z. Soumaimi[35e], D. South[48], N. Soybelman[169], S. Spagnolo[70a,70b], M. Spalla[110], D. Sperlich[54], G. Spigo[36], S. Spinali[91], D. P. Spiteri[59], M. Spousta[133], E. J. Staats[34], A. Stabile[71a,71b], R. Stamen[63a], A. Stampekis[20], M. Standke[24], E. Stanecka[87], M. V. Stange[50], B. Stanislaus[17a], M. M. Stanitzki[48], B. Stapf[48], E. A. Starchenko[37], G. H. Stark[136], J. Stark[102,aa], D. M. Starko[156b], P. Staroba[131], P. Starovoitov[63a], S. Stärz[104], R. Staszewski[87], G. Stavropoulos[46], J. Steentoft[161],

P. Steinberg[29], B. Stelzer[142,156a], H. J. Stelzer[129], O. Stelzer-Chilton[156a], H. Stenzel[58], T. J. Stevenson[146], G. A. Stewart[36], J. R. Stewart[121], M. C. Stockton[36], G. Stoicea[27b], M. Stolarski[130a], S. Stonjek[110], A. Straessner[50], J. Strandberg[144], S. Strandberg[47a,47b], M. Stratmann[171], M. Strauss[120], T. Strebler[102], P. Strizenec[28b], R. Ströhmer[166], D. M. Strom[123], L. R. Strom[48], R. Stroynowski[44], A. Strubig[47a,47b], S. A. Stucci[29], B. Stugu[16], J. Stupak[120], N. A. Styles[48], D. Su[143], S. Su[62a], W. Su[62d], X. Su[62a,66], K. Sugizaki[153], V. V. Sulin[37], M. J. Sullivan[92], D. M. S. Sultan[78a,78b], L. Sultanaliyeva[37], S. Sultansoy[3b], T. Sumida[88], S. Sun[106], S. Sun[170], O. Sunneborn Gudnadottir[161], N. Sur[102], M. R. Sutton[146], H. Suzuki[157], M. Svatos[131], M. Swiatlowski[156a], T. Swirski[166], I. Sykora[28a], M. Sykora[133], T. Sykora[133], D. Ta[100], K. Tackmann[48,t], A. Taffard[160], R. Tafirout[156a], J. S. Tafoya Vargas[66], E. P. Takeva[52], Y. Takubo[84], M. Talby[102], A. A. Talyshev[37], K. C. Tam[64b], N. M. Tamir[151], A. Tanaka[153], J. Tanaka[153], R. Tanaka[66], M. Tanasini[57a,57b], Z. Tao[164], S. Tapia Araya[137f], S. Tapprogge[100], A. Tarek Abouelfadl Mohamed[107], S. Tarem[150], K. Tariq[14a], G. Tarna[27b,102], G. F. Tartarelli[71a], P. Tas[133], M. Tasevsky[131], E. Tassi[43a,43b], A. C. Tate[162], G. Tateno[153], Y. Tayalati[35e,v], G. N. Taylor[105], W. Taylor[156b], A. S. Tee[170], R. Teixeira De Lima[143], P. Teixeira-Dias[95], J. J. Teoh[155], K. Terashi[153], J. Terron[99], S. Terzo[13], M. Testa[53], R. J. Teuscher[155,w], A. Thaler[79], O. Theiner[56], N. Themistokleous[52], T. Theveneaux-Pelzer[102], O. Thielmann[171], D. W. Thomas[95], J. P. Thomas[20], E. A. Thompson[17a], P. D. Thompson[20], E. Thomson[128], Y. Tian[55], V. Tikhomirov[37,a], Yu. A. Tikhonov[37], S. Timoshenko[37], D. Timoshyn[133], E. X. L. Ting[1], P. Tipton[172], S. H. Tlou[33g], A. Tnourji[40], K. Todome[154], S. Todorova-Nova[133], S. Todt[50], M. Togawa[84], J. Tojo[89], S. Tokár[28a], K. Tokushuku[84], O. Toldaiev[68], R. Tombs[32], M. Tomoto[84,111], L. Tompkins[143,n], K. W. Topolnicki[86b], E. Torrence[123], H. Torres[102,aa], E. Torró Pastor[163], M. Toscani[30], C. Tosciri[39], M. Tost[11], D. R. Tovey[139], A. Traeet[16], I. S. Trandafir[27b], T. Trefzger[166], A. Tricoli[29], I. M. Trigger[156a], S. Trincaz-Duvoid[127], D. A. Trischuk[26], B. Trocmé[60], C. Troncon[71a], L. Truong[33c], M. Trzebinski[87], A. Trzupek[87], F. Tsai[145], M. Tsai[106], A. Tsiamis[152,e], P. V. Tsiareshka[37], S. Tsigaridas[156a], A. Tsirigotis[152,r], V. Tsiskaridze[155], E. G. Tskhadadze[149a], M. Tsopoulou[152,e], Y. Tsujikawa[88], I. I. Tsukerman[37], V. Tsulaia[17a], S. Tsuno[84], O. Tsur[150], K. Tsuri[118], D. Tsybychev[145], Y. Tu[64b], A. Tudorache[27b], V. Tudorache[27b], A. N. Tuna[36], S. Turchikhin[57b,57a], I. Turk Cakir[3a], R. Turra[71a], T. Turtuvshin[38,x], P. M. Tuts[41], S. Tzamarias[152,e], P. Tzanis[10], E. Tzovara[100], F. Ukegawa[157], P. A. Ulloa Poblete[137c,137b], E. N. Umaka[29], G. Unal[36], M. Unal[11], A. Undrus[29], G. Unel[160], J. Urban[28b], P. Urquijo[105], P. Urrejola[137a], G. Usai[8], R. Ushioda[154], M. Usman[108], Z. Uysal[21b], V. Vacek[132], B. Vachon[104], K. O. H. Vadla[125], T. Vafeiadis[36], A. Vaitkus[96], C. Valderanis[109], E. Valdes Santurio[47a,47b], M. Valente[156a], S. Valentinetti[23b,23a], A. Valero[163], E. Valiente Moreno[163], A. Vallier[102,aa], J. A. Valls Ferrer[163], D. R. Van Arneman[114], T. R. Van Daalen[138], A. Van Der Graaf[49], P. Van Gemmeren[6], M. Van Rijnbach[125,36], S. Van Stroud[96], I. Van Vulpen[114], M. Vanadia[76a,76b], W. Vandelli[36], M. Vandenbroucke[135], E. R. Vandewall[121], D. Vannicola[151], L. Vannoli[57a,57b], R. Vari[75a], E. W. Varnes[7], C. Varni[17b], T. Varol[148], D. Varouchas[66], L. Varriale[163], K. E. Varvell[147], M. E. Vasile[27b], L. Vaslin[84], G. A. Vasquez[165], A. Vasyukov[38], F. Vazeille[40], T. Vazquez Schroeder[36], J. Veatch[31], V. Vecchio[101], M. J. Veen[103], I. Veliscek[126], L. M. Veloce[155], F. Veloso[130a,130c], S. Veneziano[75a], A. Ventura[70a,70b], S. Ventura Gonzalez[135], A. Verbytskyi[110], M. Verducci[74a,74b], C. Vergis[24], M. Verissimo De Araujo[83b], W. Verkerke[114], J. C. Vermeulen[114], C. Vernieri[143], M. Vessella[103], M. C. Vetterli[142,af], A. Vgenopoulos[152,e], N. Viaux Maira[137f], T. Vickey[139], O. E. Vickey Boeriu[139], G. H. A. Viehhauser[126], L. Vigani[63b], M. Villa[23a,23b], M. Villaplana Perez[163], E. M. Villhauer[52], E. Vilucchi[53], M. G. Vincter[34], G. S. Virdee[20], A. Vishwakarma[52], A. Visibile[114], C. Vittori[36], I. Vivarelli[146], E. Voevodina[110], F. Vogel[109], J. C. Voigt[50], P. Vokac[132], Yu. Volkotrub[86a], J. Von Ahnen[48], E. Von Toerne[24], B. Vormwald[36], V. Vorobel[133], K. Vorobev[37], M. Vos[163], K. Voss[141], J. H. Vossebeld[92], M. Vozak[114], L. Vozdecky[94], N. Vranjes[15], M. Vranjes Milosavljevic[15], M. Vreeswijk[114], R. Vuillermet[36], O. Vujinovic[100], I. Vukotic[39], S. Wada[157], C. Wagner[103], J. M. Wagner[17a], W. Wagner[171], S. Wahdan[171], H. Wahlberg[90], M. Wakida[111], J. Walder[134], R. Walker[109], W. Walkowiak[141], A. Wall[128], T. Wamorkar[6], A. Z. Wang[136], C. Wang[100], C. Wang[62c], H. Wang[17a], J. Wang[64a], R.-J. Wang[100], R. Wang[61], R. Wang[6], S. M. Wang[148], S. Wang[62b], T. Wang[62a], W. T. Wang[80], W. Wang[14a], X. Wang[14c], X. Wang[162], X. Wang[62c], Y. Wang[62d], Y. Wang[14c], Z. Wang[106], Z. Wang[51,62c,62d], Z. Wang[106], A. Warburton[104], R. J. Ward[20], N. Warrack[59], A. T. Watson[20], H. Watson[59], M. F. Watson[20], E. Watton[59,134], G. Watts[138], B. M. Waugh[96], C. Weber[29], H. A. Weber[18], M. S. Weber[19], S. M. Weber[63a], C. Wei[62a], Y. Wei[126], A. R. Weidberg[126], E. J. Weik[117], J. Weingarten[49], M. Weirich[100], C. Weiser[54], C. J. Wells[48], T. Wenaus[29], B. Wendland[49], T. Wengler[36], N. S. Wenke[110], N. Wermes[24], M. Wessels[63a], A. M. Wharton[91], A. S. White[61], A. White[8], M. J. White[1], D. Whiteson[160], L. Wickremasinghe[124], W. Wiedenmann[170], C. Wiel[50], M. Wielers[134], C. Wiglesworth[42], D. J. Wilbern[120], H. G. Wilkens[36], D. M. Williams[41], H. H. Williams[128], S. Williams[32], S. Willocq[103], B. J. Wilson[101], P. J.

Windischhofer[39], F. I. Winkel[30], F. Winklmeier[123], B. T. Winter[54], J. K. Winter[101], M. Wittgen[143], M. Wobisch[97], Z. Wolffs[114], J. Wollrath[160], M. W. Wolter[87], H. Wolters[130a,130c], A. F. Wongel[48], E. L. Woodward[41], S. D. Worm[48], B. K. Wosiek[87], K. W. Woźniak[87], S. Wozniewski[55], K. Wraight[59], C. Wu[20], J. Wu[14a,14e], M. Wu[64a], M. Wu[113], S. L. Wu[170], X. Wu[56], Y. Wu[62a], Z. Wu[135], J. Wuerzinger[110,ad], T. R. Wyatt[101], B. M. Wynne[52], S. Xella[42], L. Xia[14c], M. Xia[14b], J. Xiang[64c], M. Xie[62a], X. Xie[62a], S. Xin[14a,14e], A. Xiong[123], J. Xiong[17a], D. Xu[14a], H. Xu[62a], L. Xu[62a], R. Xu[128], T. Xu[106], Y. Xu[14b], Z. Xu[52], Z. Xu[14c], B. Yabsley[147], S. Yacoob[33a], Y. Yamaguchi[154], E. Yamashita[153], H. Yamauchi[157], T. Yamazaki[17a], Y. Yamazaki[85], J. Yan[62c], S. Yan[126], Z. Yan[25], H. J. Yang[62c,62d], H. T. Yang[62a], S. Yang[62a], T. Yang[64c], X. Yang[36], X. Yang[14a], Y. Yang[44], Y. Yang[62a], Z. Yang[62a], W-M. Yao[17a], Y. C. Yap[48], H. Ye[14c], H. Ye[55], J. Ye[14a], S. Ye[29], X. Ye[62a], Y. Yeh[96], I. Yeletskikh[38], B. K. Yeo[17b], M. R. Yexley[96], P. Yin[41], K. Yorita[168], S. Younas[27b], C. J. S. Young[36], C. Young[143], C. Yu[14a,14e,ah], Y. Yu[62a], M. Yuan[106], R. Yuan[62b], L. Yue[96], M. Zaazoua[62a], B. Zabinski[87], E. Zaid[52], Z. K. Zak[87], T. Zakareishvili[149b], N. Zakharchuk[34], S. Zambito[56], J. A. Zamora Saa[137d,137b], J. Zang[153], D. Zanzi[54], O. Zaplatilek[132], C. Zeitnitz[171], H. Zeng[14a], J. C. Zeng[162], D. T. Zenger Jr[26], O. Zenin[37], T. Ženiš[28a], S. Zenz[94], S. Zerradi[35a], D. Zerwas[66], M. Zhai[14a,14e], B. Zhang[14c], D. F. Zhang[139], J. Zhang[62b], J. Zhang[6], K. Zhang[14a,14e], L. Zhang[14c], P. Zhang[14a,14e], R. Zhang[170], S. Zhang[106], S. Zhang[44], T. Zhang[153], X. Zhang[62c], X. Zhang[62b], Y. Zhang[62c,5], Y. Zhang[96], Y. Zhang[14c], Z. Zhang[17a], Z. Zhang[66], H. Zhao[138], P. Zhao[51], T. Zhao[62b], Y. Zhao[136], Z. Zhao[62a], A. Zhemchugov[38], J. Zheng[14c], K. Zheng[162], X. Zheng[62a], Z. Zheng[143], D. Zhong[162], B. Zhou[106], H. Zhou[7], N. Zhou[62c], Y. Zhou[7], C. G. Zhu[62b], J. Zhu[106], Y. Zhu[62c], Y. Zhu[62a], X. Zhuang[14a], K. Zhukov[37], V. Zhulanov[37], N. I. Zimine[38], J. Zinsser[63b], M. Ziolkowski[141], L. Živković[15], A. Zoccoli[23a,23b], K. Zoch[61], T. G. Zorbas[139], O. Zormpa[46], W. Zou[41], L. Zwalinski[36]

[1] Department of Physics, University of Adelaide, Adelaide, Australia
[2] Department of Physics, University of Alberta, Edmonton, AB, Canada
[3] [(a)]Department of Physics, Ankara University, Ankara, Türkiye; [(b)]Division of Physics, TOBB University of Economics and Technology, Ankara, Türkiye
[4] LAPP, Université Savoie Mont Blanc, CNRS/IN2P3, Annecy, France
[5] APC, Université Paris Cité, CNRS/IN2P3, Paris, France
[6] High Energy Physics Division, Argonne National Laboratory, Argonne, IL, USA
[7] Department of Physics, University of Arizona, Tucson, AZ, USA
[8] Department of Physics, University of Texas at Arlington, Arlington, TX, USA
[9] Physics Department, National and Kapodistrian University of Athens, Athens, Greece
[10] Physics Department, National Technical University of Athens, Zografou, Greece
[11] Department of Physics, University of Texas at Austin, Austin, TX, USA
[12] Institute of Physics, Azerbaijan Academy of Sciences, Baku, Azerbaijan
[13] Institut de Física d'Altes Energies (IFAE), Barcelona Institute of Science and Technology, Barcelona, Spain
[14] [(a)]Institute of High Energy Physics, Chinese Academy of Sciences, Beijing, China; [(b)]Physics Department, Tsinghua University, Beijing, China; [(c)]Department of Physics, Nanjing University, Nanjing, China; [(d)]School of Science, Shenzhen Campus of Sun Yat-sen University, China; [(e)]University of Chinese Academy of Science (UCAS), Beijing, China
[15] Institute of Physics, University of Belgrade, Belgrade, Serbia
[16] Department for Physics and Technology, University of Bergen, Bergen, Norway
[17] [(a)]Physics Division, Lawrence Berkeley National Laboratory, Berkeley, CA, USA; [(b)]University of California, Berkeley, CA, USA
[18] Institut für Physik, Humboldt Universität zu Berlin, Berlin, Germany
[19] Albert Einstein Center for Fundamental Physics and Laboratory for High Energy Physics, University of Bern, Bern, Switzerland
[20] School of Physics and Astronomy, University of Birmingham, Birmingham, UK
[21] [(a)]Department of Physics, Bogazici University, Istanbul, Türkiye; [(b)]Department of Physics Engineering, Gaziantep University, Gaziantep, Türkiye; [(c)]Department of Physics, Istanbul University, Istanbul, Türkiye
[22] [(a)]Facultad de Ciencias y Centro de Investigaciónes, Universidad Antonio Nariño, Bogotá, Colombia; [(b)]Departamento de Física, Universidad Nacional de Colombia, Bogotá, Colombia
[23] [(a)]Dipartimento di Fisica e Astronomia A. Righi, Università di Bologna, Bologna, Italy; [(b)]INFN Sezione di Bologna, Bologna, Italy

[24] Physikalisches Institut, Universität Bonn, Bonn, Germany
[25] Department of Physics, Boston University, Boston, MA, USA
[26] Department of Physics, Brandeis University, Waltham, MA, USA
[27] [(a)]Transilvania University of Brasov, Brasov, Romania; [(b)]Horia Hulubei National Institute of Physics and Nuclear Engineering, Bucharest, Romania; [(c)]Department of Physics, Alexandru Ioan Cuza University of Iasi, Iasi, Romania ; [(d)]National Institute for Research and Development of Isotopic and Molecular Technologies, Physics Department, Cluj-Napoca, Romania; [(e)]National University of Science and Technology Politechnica, Bucharest, Romania; [(f)]West University in Timisoara, Timisoara, Romania; [(g)]Faculty of Physics, University of Bucharest, Bucharest, Romania
[28] [(a)]Faculty of Mathematics, Physics and Informatics, Comenius University, Bratislava, Slovak Republic; [(b)]Department of Subnuclear Physics, Institute of Experimental Physics of the Slovak Academy of Sciences, Kosice, Slovak Republic
[29] Physics Department, Brookhaven National Laboratory, Upton, NY, USA
[30] Universidad de Buenos Aires, Facultad de Ciencias Exactas y Naturales, Departamento de Física, y CONICET, Instituto de Física de Buenos Aires (IFIBA), Buenos Aires, Argentina
[31] California State University, CA, USA
[32] Cavendish Laboratory, University of Cambridge, Cambridge, UK
[33] [(a)]Department of Physics, University of Cape Town, Cape Town, South Africa; [(b)]iThemba Labs, Western Cape, South Africa; [(c)]Department of Mechanical Engineering Science, University of Johannesburg, Johannesburg, South Africa ; [(d)]National Institute of Physics, University of the Philippines Diliman (Philippines), Quezon City, South Africa ; [(e)]University of South Africa, Department of Physics, Pretoria, South Africa; [(f)]University of Zululand, KwaDlangezwa, South Africa; [(g)]School of Physics, University of the Witwatersrand, Johannesburg, South Africa
[34] Department of Physics, Carleton University, Ottawa, ON, Canada
[35] [(a)]Faculté des Sciences Ain Chock, Réseau Universitaire de Physique des Hautes Energies - Université Hassan II, Casablanca, Morocco; [(b)]Faculté des Sciences, Université Ibn-Tofail, Kénitra, Morocco; [(c)]Faculté des Sciences Semlalia, Université Cadi Ayyad, LPHEA-Marrakech, Morocco; [(d)]LPMR, Faculté des Sciences, Université Mohamed Premier, Oujda, Morocco; [(e)]Faculté des sciences, Université Mohammed V, Rabat, Morocco; [(f)]Institute of Applied Physics, Mohammed VI Polytechnic University, Ben Guerir, Morocco
[36] CERN, Geneva, Switzerland
[37] Affiliated with an institute covered by a cooperation agreement with CERN, Geneva, Switzerland
[38] Affiliated with an international laboratory covered by a cooperation agreement with CERN, Geneva, Switzerland
[39] Enrico Fermi Institute, University of Chicago, Chicago, IL, USA
[40] LPC, Université Clermont Auvergne, CNRS/IN2P3, Clermont-Ferrand, France
[41] Nevis Laboratory, Columbia University, Irvington, NY, USA
[42] Niels Bohr Institute, University of Copenhagen, Copenhagen, Denmark
[43] [(a)]Dipartimento di Fisica, Università della Calabria, Rende, Italy; [(b)]INFN Gruppo Collegato di Cosenza, Laboratori Nazionali di Frascati, Italy
[44] Physics Department, Southern Methodist University, Dallas, TX, USA
[45] Physics Department, University of Texas at Dallas, Richardson, TX, USA
[46] National Centre for Scientific Research "Demokritos", Agia Paraskevi, Greece
[47] [(a)]Department of Physics, Stockholm University, Stockholm, Sweden; [(b)]Oskar Klein Centre, Stockholm, Sweden
[48] Deutsches Elektronen-Synchrotron DESY, Hamburg and Zeuthen, Germany
[49] Fakultät Physik , Technische Universität Dortmund, Dortmund, Germany
[50] Institut für Kern- und Teilchenphysik, Technische Universität Dresden, Dresden, Germany
[51] Department of Physics, Duke University, Durham, NC, USA
[52] SUPA-School of Physics and Astronomy, University of Edinburgh, Edinburgh, UK
[53] INFN e Laboratori Nazionali di Frascati, Frascati, Italy
[54] Physikalisches Institut, Albert-Ludwigs-Universität Freiburg, Freiburg, Germany
[55] II. Physikalisches Institut, Georg-August-Universität Göttingen, Göttingen, Germany
[56] Département de Physique Nucléaire et Corpusculaire, Université de Genève, Genève, Switzerland
[57] [(a)]Dipartimento di Fisica, Università di Genova, Genova, Italy; [(b)]INFN Sezione di Genova, Genoa, Italy
[58] II. Physikalisches Institut, Justus-Liebig-Universität Giessen, Giessen, Germany
[59] SUPA-School of Physics and Astronomy, University of Glasgow, Glasgow, UK
[60] LPSC, Université Grenoble Alpes, CNRS/IN2P3, Grenoble INP, Grenoble, France
[61] Laboratory for Particle Physics and Cosmology, Harvard University, Cambridge, MA, USA

[62] [(a)]Department of Modern Physics and State Key Laboratory of Particle Detection and Electronics, University of Science and Technology of China, Hefei, China; [(b)]Institute of Frontier and Interdisciplinary Science and Key Laboratory of Particle Physics and Particle Irradiation (MOE), Shandong University, Qingdao, China; [(c)]School of Physics and Astronomy, Shanghai Jiao Tong University, Key Laboratory for Particle Astrophysics and Cosmology (MOE), SKLPPC, Shanghai, China; [(d)]Tsung-Dao Lee Institute, Shanghai, China
[63] [(a)]Kirchhoff-Institut für Physik, Ruprecht-Karls-Universität Heidelberg, Heidelberg, Germany; [(b)]Physikalisches Institut, Ruprecht-Karls-Universität Heidelberg, Heidelberg, Germany
[64] [(a)]Department of Physics, Chinese University of Hong Kong, Shatin, N.T., Hong Kong, China; [(b)]Department of Physics, University of Hong Kong, Hong Kong, China; [(c)]Department of Physics and Institute for Advanced Study, Hong Kong University of Science and Technology, Clear Water Bay, Kowloon, Hong Kong, China
[65] Department of Physics, National Tsing Hua University, Hsinchu, Taiwan
[66] IJCLab, Université Paris-Saclay, CNRS/IN2P3, 91405 Orsay, France
[67] Centro Nacional de Microelectrónica (IMB-CNM-CSIC), Barcelona, Spain
[68] Department of Physics, Indiana University, Bloomington, IN, USA
[69] [(a)]INFN Gruppo Collegato di Udine, Sezione di Trieste, Udine, Italy; [(b)]ICTP, Trieste, Italy; [(c)]Dipartimento Politecnico di Ingegneria e Architettura, Università di Udine, Udine, Italy
[70] [(a)]INFN Sezione di Lecce, Lecce, Italy; [(b)]Dipartimento di Matematica e Fisica, Università del Salento, Lecce, Italy
[71] [(a)]INFN Sezione di Milano, Milan, Italy; [(b)]Dipartimento di Fisica, Università di Milano, Milan, Italy
[72] [(a)]INFN Sezione di Napoli, Naples, Italy; [(b)]Dipartimento di Fisica, Università di Napoli, Naples, Italy
[73] [(a)]INFN Sezione di Pavia, Pavia, Italy; [(b)]Dipartimento di Fisica, Università di Pavia, Pavia, Italy
[74] [(a)]INFN Sezione di Pisa, Pisa, Italy; [(b)]Dipartimento di Fisica E. Fermi, Università di Pisa, Pisa, Italy
[75] [(a)]INFN Sezione di Roma, Rome, Italy; [(b)]Dipartimento di Fisica, Sapienza Università di Roma, Rome, Italy
[76] [(a)]INFN Sezione di Roma Tor Vergata, Rome, Italy; [(b)]Dipartimento di Fisica, Università di Roma Tor Vergata, Rome, Italy
[77] [(a)]INFN Sezione di Roma Tre, Rome, Italy; [(b)]Dipartimento di Matematica e Fisica, Università Roma Tre, Rome, Italy
[78] [(a)]INFN-TIFPA, Rome, Italy; [(b)]Università degli Studi di Trento, Trento, Italy
[79] Universität Innsbruck, Department of Astro and Particle Physics, Innsbruck, Austria
[80] University of Iowa, Iowa City, IA, USA
[81] Department of Physics and Astronomy, Iowa State University, Ames, IA, USA
[82] Istinye University, Sariyer, Istanbul, Türkiye
[83] [(a)]Departamento de Engenharia Elétrica, Universidade Federal de Juiz de Fora (UFJF), Juiz de Fora, Brazil ; [(b)]Universidade Federal do Rio De Janeiro COPPE/EE/IF, Rio de Janeiro, Brazil; [(c)]Instituto de Física, Universidade de São Paulo, São Paulo, Brazil; [(d)]Rio de Janeiro State University, Rio de Janeiro, Brazil
[84] KEK, High Energy Accelerator Research Organization, Tsukuba, Japan
[85] Graduate School of Science, Kobe University, Kobe, Japan
[86] [(a)]AGH University of Krakow, Faculty of Physics and Applied Computer Science, Krakow, Poland; [(b)]Marian Smoluchowski Institute of Physics, Jagiellonian University, Krakow, Poland
[87] Institute of Nuclear Physics Polish Academy of Sciences, Krakow, Poland
[88] Faculty of Science, Kyoto University, Kyoto, Japan
[89] Research Center for Advanced Particle Physics and Department of Physics, Kyushu University, Fukuoka , Japan
[90] Instituto de Física La Plata, Universidad Nacional de La Plata and CONICET, La Plata, Argentina
[91] Physics Department, Lancaster University, Lancaster, UK
[92] Oliver Lodge Laboratory, University of Liverpool, Liverpool, UK
[93] Department of Experimental Particle Physics, Jožef Stefan Institute and Department of Physics, University of Ljubljana, Ljubljana, Slovenia
[94] School of Physics and Astronomy, Queen Mary University of London, London, UK
[95] Department of Physics, Royal Holloway University of London, Egham, UK
[96] Department of Physics and Astronomy, University College London, London, UK
[97] Louisiana Tech University, Ruston, LA, USA
[98] Fysiska institutionen, Lunds universitet, Lund, Sweden
[99] Departamento de Física Teorica C-15 and CIAFF, Universidad Autónoma de Madrid, Madrid, Spain
[100] Institut für Physik, Universität Mainz, Mainz, Germany
[101] School of Physics and Astronomy, University of Manchester, Manchester, UK

[102] CPPM, Aix-Marseille Université, CNRS/IN2P3, Marseille, France
[103] Department of Physics, University of Massachusetts, Amherst, MA, USA
[104] Department of Physics, McGill University, Montreal, QC, Canada
[105] School of Physics, University of Melbourne, Victoria, Australia
[106] Department of Physics, University of Michigan, Ann Arbor, MI, USA
[107] Department of Physics and Astronomy, Michigan State University, East Lansing, MI, USA
[108] Group of Particle Physics, University of Montreal, Montreal, QC, Canada
[109] Fakultät für Physik, Ludwig-Maximilians-Universität München, Munich, Germany
[110] Max-Planck-Institut für Physik (Werner-Heisenberg-Institut), Munich, Germany
[111] Graduate School of Science and Kobayashi-Maskawa Institute, Nagoya University, Nagoya, Japan
[112] Department of Physics and Astronomy, University of New Mexico, Albuquerque, NM, USA
[113] Institute for Mathematics, Astrophysics and Particle Physics, Radboud University/Nikhef, Nijmegen, Netherlands
[114] Nikhef National Institute for Subatomic Physics and University of Amsterdam, Amsterdam, Netherlands
[115] Department of Physics, Northern Illinois University, DeKalb, IL, USA
[116] [(a)]New York University Abu Dhabi, Abu Dhabi, United Arab Emirates; [(b)]University of Sharjah, Sharjah, United Arab Emirates
[117] Department of Physics, New York University, New York, NY, USA
[118] Ochanomizu University, Otsuka, Bunkyo-ku, Tokyo, Japan
[119] Ohio State University, Columbus, OH, USA
[120] Homer L. Dodge Department of Physics and Astronomy, University of Oklahoma, Norman, OK, USA
[121] Department of Physics, Oklahoma State University, Stillwater, OK, USA
[122] Palacký University, Joint Laboratory of Optics, Olomouc, Czech Republic
[123] Institute for Fundamental Science, University of Oregon, Eugene, OR, USA
[124] Graduate School of Science, Osaka University, Osaka, Japan
[125] Department of Physics, University of Oslo, Oslo, Norway
[126] Department of Physics, Oxford University, Oxford, UK
[127] LPNHE, Sorbonne Université, Université Paris Cité, CNRS/IN2P3, Paris, France
[128] Department of Physics, University of Pennsylvania, Philadelphia, PA, USA
[129] Department of Physics and Astronomy, University of Pittsburgh, Pittsburgh, PA, USA
[130] [(a)]Laboratório de Instrumentação e Física Experimental de Partículas - LIP, Lisbon, Portugal; [(b)]Departamento de Física, Faculdade de Ciências, Universidade de Lisboa, Lisbon, Portugal; [(c)]Departamento de Física, Universidade de Coimbra, Coimbra, Portugal; [(d)]Centro de Física Nuclear da Universidade de Lisboa, Lisbon, Portugal; [(e)]Departamento de Física, Universidade do Minho, Braga, Portugal; [(f)]Departamento de Física Teórica y del Cosmos, Universidad de Granada, Granada, Spain; [(g)]Departamento de Física, Instituto Superior Técnico, Universidade de Lisboa, Lisbon, Portugal
[131] Institute of Physics of the Czech Academy of Sciences, Prague, Czech Republic
[132] Czech Technical University in Prague, Prague, Czech Republic
[133] Charles University, Faculty of Mathematics and Physics, Prague, Czech Republic
[134] Particle Physics Department, Rutherford Appleton Laboratory, Didcot, UK
[135] IRFU, CEA, Université Paris-Saclay, Gif-sur-Yvette, France
[136] Santa Cruz Institute for Particle Physics, University of California Santa Cruz, Santa Cruz, CA, USA
[137] [(a)]Departamento de Física, Pontificia Universidad Católica de Chile, Santiago, Chile; [(b)]Millennium Institute for Subatomic physics at high energy frontier (SAPHIR), Santiago, Chile; [(c)]Instituto de Investigación Multidisciplinario en Ciencia y Tecnología, y Departamento de Física, Universidad de La Serena, Chile; [(d)]Universidad Andres Bello, Department of Physics, Santiago, Chile; [(e)]Instituto de Alta Investigación, Universidad de Tarapacá, Arica, Chile ; [(f)]Departamento de Física, Universidad Técnica Federico Santa María, Valparaíso, Chile
[138] Department of Physics, University of Washington, Seattle, WA, USA
[139] Department of Physics and Astronomy, University of Sheffield, Sheffield, UK
[140] Department of Physics, Shinshu University, Nagano, Japan
[141] Department Physik, Universität Siegen, Siegen, Germany
[142] Department of Physics, Simon Fraser University, Burnaby, BC, Canada
[143] SLAC National Accelerator Laboratory, Stanford, CA, USA
[144] Department of Physics, Royal Institute of Technology, Stockholm, Sweden
[145] Departments of Physics and Astronomy, Stony Brook University, Stony Brook, NY, USA

[146] Department of Physics and Astronomy, University of Sussex, Brighton, UK
[147] School of Physics, University of Sydney, Sydney, Australia
[148] Institute of Physics, Academia Sinica, Taipei, Taiwan
[149] [(a)]E. Andronikashvili Institute of Physics, Iv. Javakhishvili Tbilisi State University, Tbilisi, Georgia; [(b)]High Energy Physics Institute, Tbilisi State University, Tbilisi, Georgia; [(c)]University of Georgia, Tbilisi, Georgia
[150] Department of Physics, Technion, Israel Institute of Technology, Haifa, Israel
[151] Raymond and Beverly Sackler School of Physics and Astronomy, Tel Aviv University, Tel Aviv, Israel
[152] Department of Physics, Aristotle University of Thessaloniki, Thessaloniki, Greece
[153] International Center for Elementary Particle Physics and Department of Physics, University of Tokyo, Tokyo, Japan
[154] Department of Physics, Tokyo Institute of Technology, Tokyo, Japan
[155] Department of Physics, University of Toronto, Toronto, ON, Canada
[156] [(a)]TRIUMF, Vancouver, BC, Canada; [(b)]Department of Physics and Astronomy, York University, Toronto, ON, Canada
[157] Division of Physics and Tomonaga Center for the History of the Universe, Faculty of Pure and Applied Sciences, University of Tsukuba, Tsukuba, Japan
[158] Department of Physics and Astronomy, Tufts University, Medford, MA, USA
[159] United Arab Emirates University, Al Ain, United Arab Emirates
[160] Department of Physics and Astronomy, University of California Irvine, Irvine, CA, USA
[161] Department of Physics and Astronomy, University of Uppsala, Uppsala, Sweden
[162] Department of Physics, University of Illinois, Urbana, IL, USA
[163] Instituto de Física Corpuscular (IFIC), Centro Mixto Universidad de Valencia-CSIC, Valencia, Spain
[164] Department of Physics, University of British Columbia, Vancouver, BC, Canada
[165] Department of Physics and Astronomy, University of Victoria, Victoria, BC, Canada
[166] Fakultät für Physik und Astronomie, Julius-Maximilians-Universität Würzburg, Würzburg, Germany
[167] Department of Physics, University of Warwick, Coventry, UK
[168] Waseda University, Tokyo, Japan
[169] Department of Particle Physics and Astrophysics, Weizmann Institute of Science, Rehovot, Israel
[170] Department of Physics, University of Wisconsin, Madison, WI, USA
[171] Fakultät für Mathematik und Naturwissenschaften, Fachgruppe Physik, Bergische Universität Wuppertal, Wuppertal, Germany
[172] Department of Physics, Yale University, New Haven, CT, USA

[a] Also Affiliated with an institute covered by a cooperation agreement with CERN, Geneva, Switzerland
[b] Also at An-Najah National University, Nablus, Palestine
[c] Also at Borough of Manhattan Community College, City University of New York, New York, NY, USA
[d] Also at Center for High Energy Physics, Peking University, China
[e] Also at Center for Interdisciplinary Research and Innovation (CIRI-AUTH), Thessaloniki, Greece
[f] Also at Centro Studi e Ricerche Enrico Fermi, Rome, Italy
[g] Also at CERN, Geneva, Switzerland
[h] Also at Département de Physique Nucléaire et Corpusculaire, Université de Genève, Genève, Switzerland
[i] Also at Departament de Fisica de la Universitat Autonoma de Barcelona, Barcelona, Spain
[j] Also at Department of Financial and Management Engineering, University of the Aegean, Chios, Greece
[k] Also at Department of Physics, Ben Gurion University of the Negev, Beer Sheva, Israel
[l] Also at Department of Physics, California State University, Sacramento, USA
[m] Also at Department of Physics, King's College London, London, UK
[n] Also at Department of Physics, Stanford University, Stanford, CA, USA
[o] Also at Department of Physics, University of Fribourg, Fribourg, Switzerland
[p] Also at Department of Physics, University of Thessaly, Thessaly, Greece
[q] Also at Department of Physics, Westmont College, Santa Barbara, USA
[r] Also at Hellenic Open University, Patras, Greece
[s] Also at Institucio Catalana de Recerca i Estudis Avancats, ICREA, Barcelona, Spain
[t] Also at Institut für Experimentalphysik, Universität Hamburg, Hamburg, Germany
[u] Also at Institute for Nuclear Research and Nuclear Energy (INRNE) of the Bulgarian Academy of Sciences, Sofia, Bulgaria

[v] Also at Institute of Applied Physics, Mohammed VI Polytechnic University, Ben Guerir, Morocco
[w] Also at Institute of Particle Physics (IPP), Toronto, Canada
[x] Also at Institute of Physics and Technology, Mongolian Academy of Sciences, Ulaanbaatar, Mongolia
[y] Also at Institute of Physics, Azerbaijan Academy of Sciences, Baku, Azerbaijan
[z] Also at Institute of Theoretical Physics, Ilia State University, Tbilisi, Georgia
[aa] Also at L2IT, Université de Toulouse, CNRS/IN2P3, UPS, Toulouse, France
[ab] Also at Lawrence Livermore National Laboratory, Livermore, USA
[ac] Also at National Institute of Physics, University of the Philippines Diliman (Philippines), Quezon City, Philippines
[ad] Also at Technical University of Munich, Munich, Germany
[ae] Also at The Collaborative Innovation Center of Quantum Matter (CICQM), Beijing, China
[af] Also at TRIUMF, Vancouver, BC, Canada
[ag] Also at Università di Napoli Parthenope, Naples, Italy
[ah] Also at University of Chinese Academy of Sciences (UCAS), Beijing, China
[ai] Also at Department of Physics, University of Colorado Boulder, Colorado, USA
[aj] Also at Washington College, Chestertown, MD, USA
[ak] Also at Physics Department, Yeditepe University, Istanbul, Türkiye
[*] Deceased